

# Mitochondrial-Nuclear Interactions Mediate Sex-Specific Transcriptional Profiles in *Drosophila*

Jim A. Mossman,<sup>\*,1</sup> Jennifer G. Tross,<sup>\*,†,§</sup> Nan Li,<sup>\*\*</sup> Zhijin Wu,<sup>\*\*</sup> and David M. Rand<sup>\*,1</sup>

<sup>\*</sup>Department of Ecology and Evolutionary Biology, and <sup>\*\*</sup>Department of Biostatistics, Brown University, Providence, Rhode Island 02912, <sup>†</sup>Department of Medical Oncology, and <sup>‡</sup>Department of Biostatistics and Computational Biology, Dana-Farber Cancer Institute, Boston, Massachusetts 02215, <sup>§</sup>Harvard-MIT Division of Health Sciences and Technology, Harvard Medical School, Boston, Massachusetts 02115

ORCID ID: 0000-0001-6817-3459 (D.M.R.)

**ABSTRACT** The assembly and function of mitochondria require coordinated expression from two distinct genomes, the mitochondrial DNA (mtDNA) and nuclear DNA (nDNA). Mutations in either genome can be a source of phenotypic variation, yet their coexpression has been largely overlooked as a source of variation, particularly in the emerging paradigm of mitochondrial replacement therapy. Here we tested how the transcriptome responds to mtDNA and nDNA variation, along with mitonuclear interactions (mtDNA × nDNA) in *Drosophila melanogaster*. We used two mtDNA haplotypes that differ in a substantial number of single nucleotide polymorphisms, with >100 amino acid differences. We placed each haplotype on each of two *D. melanogaster* nuclear backgrounds and tested for transcription differences in both sexes. We found that large numbers of transcripts were differentially expressed between nuclear backgrounds, and that mtDNA type altered the expression of nDNA genes, suggesting a retrograde, *trans* effect of mitochondrial genotype. Females were generally more sensitive to genetic perturbation than males, and males demonstrated an asymmetrical effect of mtDNA in each nuclear background; mtDNA effects were nuclear-background specific. mtDNA-sensitive genes were not enriched in male- or female-limited expression space in either sex. Using a variety of differential expression analyses, we show the responses to mitonuclear covariation to be substantially different between the sexes, yet the mtDNA genes were consistently differentially expressed across nuclear backgrounds and sexes. Our results provide evidence that the main mtDNA effects can be consistent across nuclear backgrounds, but the interactions between mtDNA and nDNA can lead to sex-specific global transcript responses.

**KEYWORDS** mtDNA; epistasis; *Drosophila*; transcriptome; mitonuclear; retrograde signaling

**T**HE ancient symbiosis that led to current day mitochondria and their eukaryotic host was a major milestone for inter-genomic communication (Sagan 1967; Martin and Muller 1998). During the following ~2 billion years, the resulting eukaryotic cell consolidated the genetic information from two ancestral genomes to a reduced set of genes in the mitochondrial organelle [mitochondrial DNA (mtDNA)] and many nuclear-encoded genes that are required for mitochondrial function. At ~16.5 kb in size, the mtDNA encodes 13

oxidative phosphorylation (OXPHOS) proteins, 22 transfer RNAs (tRNAs), and 2 ribosomal RNAs (Taanman 1999). The remaining ~1200 proteins associated with mitochondria are encoded by the nucleus (Wallace 1999). Mitochondria therefore require coordinated expression of genes from both mitochondrial and nuclear genomes for efficient function (Rand 2001; Smeitink *et al.* 2001). Crucially, the effects of mtDNA variation, nuclear DNA (nDNA) variation, and their interactions on gene expression are poorly understood, yet they are expected to play a large role in an organism's response to environmental or cellular stress.

Mitochondria perform many functions in the cell other than ATP production, including maintaining homeostasis, regulating redox signaling, and apoptosis (Friedman and Nunnari 2014). Recent studies have shown that when mitochondrial function is perturbed, retrograde signaling to the nucleus occurs via the unfolded protein response (UPR) (Houtkooper *et al.* 2013; Quiros *et al.* 2016), however the role of underlying mitonuclear

Copyright © 2016 by the Genetics Society of America

doi: 10.1534/genetics.116.192328

Manuscript received June 5, 2016; accepted for publication August 17, 2016; published Early Online August 24, 2016.

Available freely online through the author-supported open access option.

Supplemental material is available online at [www.genetics.org/lookup/suppl/doi:10.1534/genetics.116.192328/-/DC1](http://www.genetics.org/lookup/suppl/doi:10.1534/genetics.116.192328/-/DC1).

<sup>1</sup>Corresponding authors: Department of Ecology and Evolutionary Biology, Box G, Brown University, Providence, RI 02912. E-mail: Jim\_Mossman@brown.edu; and david\_rand@brown.edu

genetic variation in retrograde signaling has not been studied in the context of gene expression. Aberrations in mitochondrial function are known to cause a wide spectrum of disorders in humans (DiMauro and Schon 2003; Lin and Beal 2006), and mitochondrial diseases with an mtDNA component can be difficult to characterize due to the complexity of dual genomic organization and large numbers of intergenomic interactions. The relatively high mutation rate, lack of protective histones, maternal inheritance, reduced effective population size, and no recombination all contribute to a higher frequency of deleterious mutations in mtDNA (Gemmell *et al.* 2004). These “natural” genetic variants segregate together in complete linkage disequilibrium in the form of mtDNA haplotypes. Importantly, both *de novo* (spontaneous) mutations and haplotype variation have been associated with disease phenotypes across a number of species (Roubertoux *et al.* 2003; DiMauro and Davidzon 2005).

While specific mtDNA mutations—associated with haplotype variation—increase the risks of some diseases, *e.g.*, neurodegenerative diseases and aging (Stewart and Chinnery 2015), they do not operate in isolation from the substantial nuclear-encoded contribution to mitochondrial phenotypes (Wallace 1999; Wong 2012). Deleterious mitochondrial mutations often demonstrate incomplete penetrance (Giordano *et al.* 2014), suggesting nuclear variants may dampen or amplify their effects. An unknown proportion of phenotypes demonstrating missing heritability are likely to involve the interactions (epistases) between mtDNA and nDNA (Mossman *et al.* 2016). Indeed, mitonuclear interactions have been largely overlooked as sources of phenotypic variation (Pesole *et al.* 2012), even though recent studies have shown mitonuclear interactions to be pervasive and context dependent in a suite of life history traits (Hoekstra *et al.* 2013; Mossman *et al.* 2016).

mtDNA variation is hypothesized to affect males more severely than females due to an imbalance in the strength of purifying selection between the sexes (Frank and Hurst 1996). Because mtDNAs are maternally inherited, males are at a genetical dead end for mtDNA evolution. Mutations that have negligible or zero effects in females, yet severe effects in males, can rise to high frequencies in populations by genetic drift (Frank and Hurst 1996). Under this hypothesis, it is predicted that mtDNA variation should promote larger phenotypic effects in males than females. Initial support for this hypothesis was suggested by mitochondrial disease cases that appeared more severe in males than females (Wallace 1992; Bernes *et al.* 1993; Casademont *et al.* 1994). More recent studies provide support for the Frank and Hurst hypothesis in *Drosophila* aging (Camus *et al.* 2012) and fertility (Yee *et al.* 2013; but see Friberg and Dowling 2008), yet there is a robust absence of support in development time and viability (egg-to-adult survival) (Mossman *et al.* 2016). In humans, there is also equivocal evidence for the role of mtDNA haplotypes in fertility-related traits in males (Ruiz-Pesini *et al.* 2000; Pereira *et al.* 2007; Mossman *et al.* 2012). There is some evidence in *Drosophila* that sex-specific mtDNA effects on gene expression exist (Innocenti *et al.* 2011), and

that variation in male-limited gene expression is dominated by mtDNA variation. However, it is not known whether differential gene expression associated with mtDNA variation is a robust phenotype across nuclear genetic backgrounds.

Here, we use a *Drosophila* mitonuclear introgression model (Montooth *et al.* 2010; Meiklejohn *et al.* 2013; Villa-Cuesta *et al.* 2014; Holmbeck *et al.* 2015) to test the hypotheses that mtDNA variation, nDNA variation, and mtDNA  $\times$  nDNA interactions impact gene expression in males and females. A main motivation of this experiment was to examine whether different mitonuclear genotypes have distinct gene expression profiles. Here, we focused on a  $2 \times 2$  genotype table (*sensu* Roubertoux *et al.* 2003) to elucidate whether mtDNA variation *per se*, nuclear variation *per se*, and mitochondrial  $\times$  nuclear variation influences gene expression in a sex-specific manner.

We have previously shown that across several *Drosophila* Genetic Reference Panel nuclear backgrounds, the *sil* and *OreR* mtDNA haplotypes diverge in phenotypic values (development time, egg-to-adult viability) (Mossman *et al.* 2016). We have also shown there are nucleotide substitutions between *sil* and *OreR* mtDNAs that have putative deleterious effect on protein function (Mossman *et al.* 2016), motivating an examination of gene expression variation that is associated with mtDNA and nuclear variation. We hypothesized that mtDNA variation preferentially modifies the expression of mitochondria-associated OXPHOS genes from both mitochondrial and nuclear genomes. Furthermore, we wanted to characterize the cellular processes and functional categories of genes that are modified by mtDNA, nuclear, and mitonuclear variation. We further hypothesized that mitochondrial protein translational machinery (Jacobs and Turnbull 2005) would be largely influenced due to its critical role in protein synthesis and the key participation of mitochondrial ribosomes. Finally, we investigated whether genes differentially expressed by mtDNA variation were enriched in male-limited genes (*e.g.*, those involved in testes and sperm-related proteins) to test the generality of the Frank and Hurst hypothesis in alternative nuclear backgrounds.

## Materials and Methods

### Mitonuclear panel

Experiments were performed on four genotypes whose nuclear genomes were introgressed with mtDNAs from two sources: (i) *OregonR* strain of *Drosophila melanogaster* and (ii) *sil* strain of *D. simulans*. The nuclear backgrounds were *Oregon R* (*OreR*) and *Austria W132* (*AutW132*), which are both *D. melanogaster* nuclear types. The four genotypes were (mito; nuclear): (i) *OreR*; *OreR*, (ii) *OreR*; *AutW132*, (iii) *sil*; *OreR*, and (iv) *sil*; *AutW132*. Specifically, the introgressions were performed by balancer chromosome replacement, followed by backcrossing to the original stock to homogenize the nuclear background and remove nuclear variation that may have been retained in the chromosome replacement process. The full double balancer replacement scheme is

described in Montooth *et al.* (2010). Alignments between mtDNA coding regions reveal substantial sequence divergence between *OreR* (NC\_001709) and *siI* (AF00835) mtDNA haplotypes: a pairwise amino acid divergence (103 amino acids) and a pairwise synonymous divergence (418 SNPs) (Montooth *et al.* 2010).

All strains used in this study were cleared of *Wolbachia* using tetracycline, and *Wolbachia* negative status was confirmed by PCR (Montooth *et al.* 2010).

### **RNA sequencing sample preparation**

Prior to RNA extraction, flies were reared on standard laboratory food at 25° on a 12 hr light:12 hr dark cycle, and density-controlled for one generation (five males and five females per vial). After density control, eclosed flies were allowed to mate for 3 days on standard food and were then separated by sex at a density of 50 males or 50 females per vial. After 2 days of recovery from CO<sub>2</sub> anesthesia, batches of flies were transferred into a 1.5-ml microcentrifuge tube and immediately flash frozen in liquid nitrogen.

RNA was extracted from 30, 5-day-old whole healthy flies in each genotype by sex treatment. We used whole flies to test whether sex-limited gene expression was associated with mtDNA and nDNA genetic effects, as found by Innocenti *et al.* (2011). In addition, a number of other studies of genetic variation for gene expression in *Drosophila* have used whole flies, allowing for more direct comparison with our results (Gibson *et al.* 2004; Ayroles *et al.* 2009; Huang 2012; Mackay *et al.* 2012; Huang *et al.* 2014). In males, there were three replicates per genotype and in females there were three replicates in all genotypes apart from the *siI*; *AutW132*, which had two replicates. We followed a modified RNA sequencing (RNA-seq) sample preparation protocol from the Gilad Laboratory (Chicago University; [http://giladlab.uchicago.edu/data/RNASeq\\_v2%202.doc](http://giladlab.uchicago.edu/data/RNASeq_v2%202.doc)). Messenger RNA (mRNA) was first extracted, followed by RNA fragmentation, complementary DNA (cDNA) first strand synthesis, second strand synthesis, end repair, poly adenylation, adapter ligation, and PCR enrichment. Throughout, RNA and DNA were quantified using the Qubit Kits (RNA Broad Range, dsDNA Broad Range, and dsDNA High Sensitivity) with a Qubit 1.0 Fluorometer. All Qubit reagents were obtained from Molecular Probes (Eugene, OR). Following PCR enrichment, we size selected PCR products with size range of 334–500 bp using a Caliper LabChip XT (DNA 750 chip) (Caliper Life Sciences, Hopkington, MA).

### **Gene expression assays**

Gene expression was assayed in both sexes in all four genotypes using Illumina RNA-seq (HiSeq; Illumina, San Diego) with a 50-bp, single-end protocol. Samples were processed at Brown University's Genomics Core Facility using an Illumina HiSeq2000 platform.

### **RNA-seq data preprocessing**

RNA-seq read quality was first assessed using the FastQC v0.11.5 program (<http://www.bioinformatics.babraham.ac.uk/projects/fastqc/>).

We then filtered the reads using a FASTQ quality filter (`fastq_quality_filter`) with `-q 20` and `-p 80` flags, as implemented in the FASTX-Toolkit ([http://hannonlab.cshl.edu/fastx\\_toolkit/commandline.html#fastq\\_quality\\_filter\\_usage](http://hannonlab.cshl.edu/fastx_toolkit/commandline.html#fastq_quality_filter_usage)). These values correspond to removing reads with 80% bases having a quality score of <20. Adapters were clipped from the reads using the `fastx_clipper` tool in the FASTX-Toolkit ([http://hannonlab.cshl.edu/fastx\\_toolkit/commandline.html#fastx\\_clipper\\_usage](http://hannonlab.cshl.edu/fastx_toolkit/commandline.html#fastx_clipper_usage)) and FastQC was repeated. We used TopHat v2.0.12 (<https://ccb.jhu.edu/software/tophat/index.shtml>) (Trapnell *et al.* 2012) with Bowtie2 v2.2.3 (<http://bowtie-bio.sourceforge.net/index.shtml>) to map the reads to the dm3 reference genome using the dm3flybase.gtf annotation file obtained from the University of California Santa Cruz Genome Browser (<https://genome.ucsc.edu/>). BAM files generated by TopHat were converted to SAM files using SAMtools (<http://samtools.sourceforge.net/>) (Li *et al.* 2009), and reads mapping to specific genome features (genes) were counted using `htseq-count` (<http://www-huber.embl.de/users/anders/HTSeq/doc/count.html>) (Anders *et al.* 2015). The read-count data table obtained via HTSeq was used for downstream analyses. All preprocessing was conducted using computational resources and services at the Center for Computation and Visualization, Brown University.

### **RNA-seq data analysis**

Differential expression (DE) analyses were conducted using two methods: DESeq (Anders and Huber 2010) following the vignette workflow (<http://bioconductor.org/packages/release/bioc/vignettes/DESeq/inst/doc/DESeq.pdf>), and edgeR (Robinson *et al.* 2010). We also used a clustering algorithm to categorize genes based on their between-genotype expression profiles (see below). The measurement accuracy of RNA-seq was validated using a subset of genes and quantitative PCR (qPCR) as described in detail in Supplemental Material, File S1 (see also Table S1; Figure S13).

### **Gene filtering**

In total we analyzed data generated from 23 RNA-seq libraries (11 female, 12 male). Throughout the data analyses, we used both complete data sets (including all genes), and filtered data (excluding the lowest 40th percentile of the data *sensu* the recommendations in the DESeq vignette). The purpose of the independent filtering was to remove genes from the total data set that have little or no chance of showing significant evidence of DE, while simultaneously increasing the detection power with a similar false discovery rate (FDR) (Bourgon *et al.* 2010). We specify in each *Results* section which data set (unfiltered or filtered) and which analysis program was used.

### **Gene clustering**

We used four genotypes in total for this study and our primary aim was to detect genes that show expression profiles consistent with mtDNA effects, nDNA effects, and mtDNA × nucDNA (epistatic) effects. We rationalized that different

genetic effects would produce different norms of reaction shapes (profiles) across genotypes. We aimed to cluster genes based on their expression across different genotypes. For example, for all genotypes (independent variable), we asked which genes segregated with a similar pattern, and which of those patterns correspond with nuclear effects, mtDNA effects, and their mtDNA  $\times$  nDNA interactions (see Figure S1 for theoretical gene expression outlines).

Model-based clustering of gene expression profiles was performed using MBClusterSeq (Si *et al.* 2014), with  $k = 20$  clusters in both sexes. Negative binomial (NB) models were used to perform the hierarchical clustering and hybrid tree builds as implemented in the MBClusterSeq package. Clusters are described using interaction plots of individual genes in each cluster and the mean genotype values per cluster were calculated. The log-fold change is relative to the normalized gene expression across all treatments (genotypes) with each row of the log-fold change matrix having a zero sum. The clustering algorithm allocates genes to a group based on their gene expression profile (in this case, the shape of the gene expression–genotype relationship).

### Gene ontology enrichment

Gene ontology (GO) enrichment analyses were performed on clustered genes using the Bioprofiling.de program (<http://bioprofiling.de/>) (Antonov 2011) and the GO Consortium database (<http://geneontology.org/>) with the default submission and “*Drosophila melanogaster*” organism selected. The outputs of the “ProfCom\_GO” analyses (Antonov *et al.* 2008) were filtered for GO categories that evidenced a Bonferroni-corrected  $P$ -value of  $<0.05$  and these GO categories were used in the heat map construction. In the sex-specific gene expression analysis, we used GOrilla GO enrichment (Eden *et al.* 2009) to investigate the GO processes that were enriched in the male- and female-biased gene sets.

### Analyses of OXPHOS gene subset

In addition to the analyses of the global gene set, genes encoding OXPHOS-related proteins (complexes I, II, III, IV, and ATP synthase) were selected for closer examination because these are putative targets of mitochondrial variation. Both mtDNA and nuclear genes targeted to the mitochondrion were downloaded from the MitoDrome database (Sardiello *et al.* 2003; D’Elia *et al.* 2006). Arc diagrams were used to display the relationship between various genes in the OXPHOS pathway in *D. melanogaster* (Tripoli *et al.* 2005) and the effect of alternative mtDNA haplotype in each nuclear background and in each sex. DE was judged by DESeq in each nuclear background and sex separately. For clarity, only genes with a  $P$ -value of  $<0.1$  are shown and a gene was only required to be included in one sex or nuclear background to be present in the arc diagram. A total of 78 nuclear genes and 13 mtDNA genes were included in the initial screen, of which 53 genes were included in the visualization (11 mtDNA genes and 42 nuclear genes;  $P < 0.1$  in at least one genetic background).

### Data availability

*Drosophila* strains used in this study are available upon request. FASTQ files from the 23 RNA-seq libraries are available at the Sequence Read Archive (SRA) under project accession SRP082430.

## Results

### Between-sex gene expression correlations

We first investigated whether there were signatures of sex-specific gene expression as a basis for understanding how mtDNAs may or may not modify gene expression in a sex-specific manner. Figure 1, A–D, shows biplots of the four mitonuclear genotypes using pseudocounts of the unfiltered data set. The pseudocount transformation is  $\log_2(\text{read count} + 1)$ , and was calculated using the base mean in DESeq. There are clear gene subsets in the data distributions that show sex-biased expression, particularly for male-biased genes (Figure 1). The numbers of genes that are common across genotypic intersections are described for each sex (females, Figure 1E; males, Figure 1F). The female- and male-biased genes (red and blue data in Figure 1, A–D, respectively) were intersected separately and those elements that were common to all four genotypes were subjected to GO-enrichment analysis. GO-enrichment analyses (Eden *et al.* 2009) show male-biased genes are enriched for sperm-related processes (Figure 1F and Table 1). Genes with female-biased expression (shown as red in Figure 1) are associated with, among other processes, egg-related GO categories. Table 1 describes the male-specific enrichment of GO categories.

### Genotype signatures of gene expression

There are large differences between the sexes in genotype signatures of gene expression. Figure 2 shows multidimensional scaling (MDS) plots (Ritchie *et al.* 2015) of each genotype in female and male data sets. The data are plotted in two dimensions and the distances between samples (libraries) approximately reflect the leading  $\log_2$ -fold change between the samples for the genes that distinguish those samples (Ritchie *et al.* 2015). Data were filtered as the top 10,000, top 1000, top 100, and top 10 genes. The top genes are those with the largest SD in expression between samples. In females, the progressive filtering increases the genotype-genotype distance, whereas in males, the progressive filtering increased the distance between mitochondrial genotypes only in the *Aut132* nuclear background (Figure 2).

### mtDNA substitution effects

We next tested whether mtDNA substitution conferred DE of genes in each nuclear background and in both sexes, separately. We did this using DESeq (Anders and Huber 2010) on individual nuclear backgrounds for each sex (two tests per sex). The read-count data were modeled using NB distributions. The fold change and associated  $P$ -value were calculated for each gene and  $P$ -values were adjusted to account



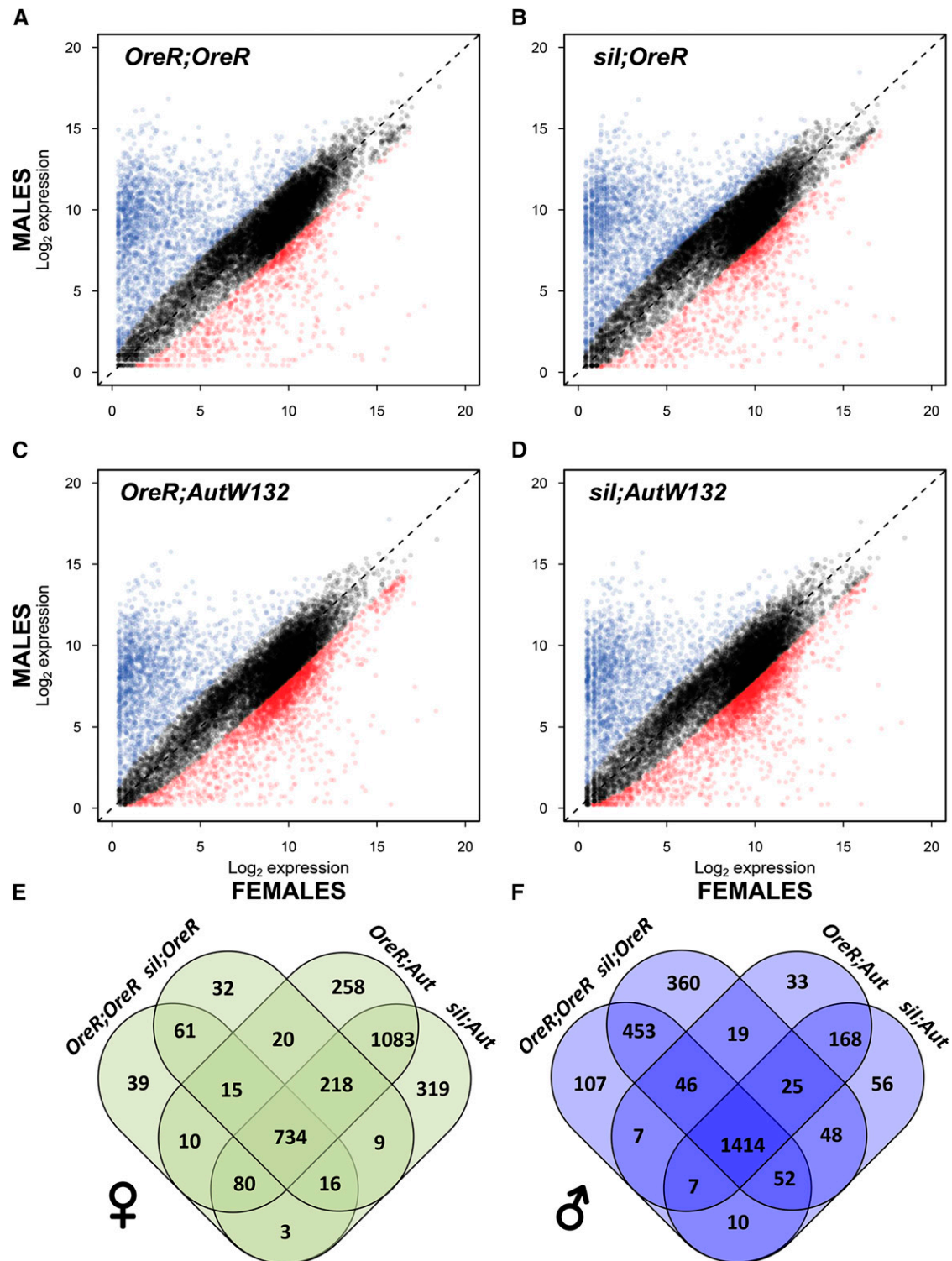


**Figure 1** Sex-biased gene expression across four mitonuclear genotypes. Gene expression profiles of individual genes are shown for each genotype analyzed in this study: (A) *OreR;OreR*, (B) *sil;OreR*, (C) *OreR;AutW132*, and (D) *sil;AutW132*. Biplots show female gene expression on the abscissa with corresponding male gene expression values on the ordinal scale. Data highlighted in red and blue show female- and male-biased genes, respectively. Sex bias was determined as a  $\log_2$ -fold  $>2$  difference between females and males. Data in black show no sex bias in expression. (E and F) Venn diagrams describe the number of genes that are intersected between genotypes for sex-biased expression (red and blue genes in A–D). (E) Female and (F) male intersections are shown. Generally, there were more intersected genes that demonstrated male-biased expression than female-biased expression. Genes at the four-genotype intersection were subject to GO analysis. Male-specific GO processes are described in Table 1.

**Table 1 Male-biased gene expression**

GO term	Description	No. genes	Enrichment	Adjusted <i>P</i> -value
GO:0032504	Multicellular organism reproduction	75	3.58	1.82e−20
GO:0000003	Reproduction	75	3.43	1.75e−19
GO:0046692	Sperm competition	17	6.34	5.37e−08
GO:0044706	Multi-multicellular organism process	17	6.12	9.30e−08
GO:0048232	Male gamete generation	33	2.89	1.45e−05
GO:0007283	Spermatogenesis	32	2.83	3.60e−05
GO:0003341	Cilium movement	12	6.04	4.64e−05
GO:0048515	Spermatid differentiation	10	5.6	1.47e−03

Significantly enriched GO categories are shown for the genes that are intersected between all four mitonuclear genotypes. *P*-values were adjusted using the Benjamini and Hochberg (1995) method.

for multiple testing using the Benjamini–Hochberg method (Benjamini and Hochberg 1995), providing FDRs. In all cases the *Oregon R* mtDNA was the reference mtDNA background and effects of the *sil* haplotype are reported in the analyses. For nDNA results, the *OregonR* nDNA was the reference and the reported fold changes are for *AutW132/OregonR*.

In both females and males, mtDNA substitution conferred DE of genes from both mtDNA and nuclear genomes (Figure 3). In general, the response to mtDNA substitution was greater in females than males. Both sexes and nuclear backgrounds responded with distinct patterns. Among the most consistently modified genes were those encoded by mtDNA, with *sil* haplotypes mainly conferring downregulation in gene expression relative to the *OregonR* baseline. The majority of mtDNA OXPHOS protein-coding genes were downregulated (comparison = *sil/OreR*) in both males and females and in both nuclear backgrounds, with exceptions for mtDNA *ND2*, which was consistently upregulated across sexes and nuclear backgrounds.

Volcano plots in Figure 3 describe the effects of mtDNA substitution. Shown are the results of DESeq analyses for the unfiltered data set. The results for the filtered data set (top 60% quantile) are shown in Figure S2. In the unfiltered- and filtered-gene analyses, estimation of size factors to normalize the counts to a common scale was performed on the unfiltered and filtered data, respectively.

We then intersected the genes that were significantly differentially expressed by mtDNA substitution in each nuclear background (×2) and in both sexes (×2). In this analysis, we did not require a specific direction of effect, e.g., up- or down-regulated, just that the genes were present at a *P*-value threshold. A summary of the number of genes that are present, at various *P*-value thresholds, are shown in Figure S3. Those genes that are consistently differentially expressed (at *P* < 0.05) by mtDNA substitution across nuclear backgrounds and sexes are described in Table 2. Specifically, we report a conservative analysis in which all four nuclear background × sex treatments are intersected (A∩B∩C∩D)—where ∩ signifies intersection—and a more parsimonious analysis, in which a gene was only required to be included in a three-way intersection, e.g., including A∩B∩C, A∩B∩D, A∩C∩D, and B∩C∩D (Table 2). In the strict four-genotype intersection, only five genes were significantly differentially expressed by mtDNA variation in (A) female *OregonR* background, (B) fe-

male *AutW132* background, (C) male *OregonR* background, and (D) male *AutW132* backgrounds. These were three mtDNA genes (*ND2*, *ATP6ase*, and *ND4L*), an unannotated computed gene (*CG11966*), and *Jonah 25Bi* (*Ser4*; a serine protease). High within-group variance that results from pooling across other experimental factors (e.g., nuclear backgrounds) is likely to reduce the sensitivity to detect first-order effects of mtDNA, so the five core genes influenced by mtDNA variation is likely a conservative estimate of the true number.

#### Mitochondrial OXPHOS genes and mtDNA variation

mtDNA variation conferred different effects on global gene expression between the sexes and nuclear backgrounds (Figure 3). We next focused on the nuclear and mtDNA genes of the OXPHOS pathway, since these are jointly encoded by mtDNA and nuclear genes and hypothesized to be more sensitive to mtDNA and nuclear covariation. We filtered our global DE data sets for the OXPHOS genes and graphed those genes that were differentially expressed (Figure 4). We divided the genes into their respective OXPHOS complexes.

In males, there was a high degree of symmetry in the effects of mtDNA variation across the nuclear backgrounds (Figure 4). The differentially expressed genes (with *P* < 0.05) were exclusively targeted to mtDNA-encoded proteins within the various complexes (red gene identifiers in Figure 4) across both *OregonR* and *AutW132* nuclear backgrounds. In the *AutW132* nuclear background, fewer mtDNA OXPHOS genes achieved significance, particularly those in complex IV. In addition, several genes were consistently differentially expressed across nuclear backgrounds, including *CG34092* (*ND1*), *CG34063* (*ND2*), *CG34076* (*ND3*), *CG34086* (*ND4L*), *CG34090* (*CytB*), and *CG34073* (*ATPase6*).

In females the patterns were different and a much larger suite of OXPHOS-associated genes were differentially expressed from both mtDNA and nuclear-encoded genes. This effect was mainly isolated to the *AutW132* nuclear background, which demonstrated a high degree of DE driven by alternative mtDNAs. In *AutW132*, genes that were differentially expressed in males were more significantly differentially expressed in females. The opposite effect is evident in the *OregonR* nuclear background, in which only a small number of OXPHOS-associated genes were differentially expressed in females.

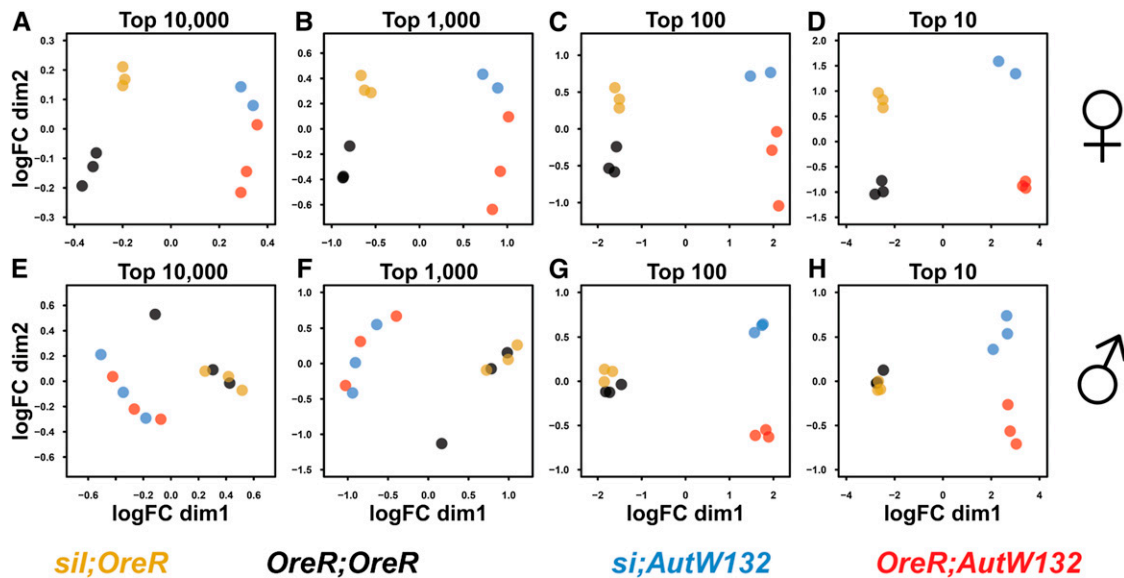


**Figure 2** Genotype signatures of transcript variation. MDS plots show progressive filtering of genes based on their expression differences. The distance between points in a plot approximately reflects the relatedness between libraries based on their transcript measures. (A–D) Female and (E–H) male profiles are shown. The top 10,000 (A, E), top 1000 (B, F), top 100 (C, G), and top 10 (D, H) most deviant genes are shown. Separate genotypes are color coded: *sil;OreR*, yellow; *OreR;OreR*, black; *sil;AutW132*, blue; *OreR;AutW132*, red. Mitonuclear genotypes were clearly distinguishable across all filtering levels in females. Only the most differentially expressed genes were able to distinguish mtDNA haplotypes in males.

### Global gene expression and mtDNA substitution

The different patterns we observed between males and females in the OXPHOS gene subset suggest the relationships between gene expression and mtDNA substitution differs between the sexes. To investigate whether this effect is evident at a global gene-expression level, we plotted the  $\log_2$ -fold change in gene expression between *sil* and *OregonR* mtDNAs for each nuclear background within each sex (Figure 5). We found there were dramatic differences between the sexes in the patterns of  $\log_2$ -fold change; the majority of genes were significantly positively correlated in females (global gene correlation  $r = +0.14$ ,  $t = 16.42$ , d.f. = 12,623,  $P < 2.2e-16$ ), but negatively correlated in males ( $r = -0.12$ ,  $t = -13.99$ , d.f. = 13,165,  $P < 2.2e-16$ ). Notably, the mtDNA genes (highlighted in Figure 5) were consistently positively correlated between nuclear backgrounds in both sexes (females:  $r = +0.97$ ,  $t = 12.56$ , d.f. = 11,  $P = 7.279e-08$ ; males:  $r = +0.86$ ,  $t = 5.51$ , d.f. = 11,  $P = 0.0002$ ). Figure 5 shows the results for the unfiltered data set. The plots of the filtered data are shown in Figure S4. In both sexes, the genes from OXPHOS complex IV and ATP synthase are generally clustered together and this may reflect their stoichiometric dependence and strict regulation. Complex I genes, by contrast, demonstrate wide variation in  $\log_2$ -fold change as a result of mtDNA substitution. The CG34063 (*ND2*) gene is the only gene that is consistently upregulated in both nuclear backgrounds and in both sexes as a result of mtDNA substitution. For the mtDNA OXPHOS genes, the *ND2* gene was consistently ranked as the highest upregulated  $\log_2$ -fold change and *ND3* was consistently the lowest ranked (highest negative  $\log_2$ -fold change).

### Clustering genes by between-genotype expression profiles

Using a clustering approach, we identified subsets of genes from the global distribution that demonstrated distinct expression patterns across the four genotypes. Theoretical profiles corresponding with mtDNA, nDNA, and mtDNA  $\times$  nDNA interactions are described in Figure S1. In total, we produced  $k = 20$  clusters for each sex and the filtered data set was used, since a large number of genes in the unfiltered data have zero read counts. Hybrid tree topologies and clusters are shown for females and males in Figure S5 and Figure S6, respectively. We identified a number of clusters that were consistent with first-order nuclear effects in both females and males (Figure 6 and Figure S7, respectively). Clear mtDNA effects were only apparent in the female data set and males showed very little evidence of mtDNA effects (see above).

Males showed an overwhelming enrichment of mitonuclear interactions across gene clusters (Figure S7). The effects of mtDNA substitution are largely in opposite directions in the alternative nuclear backgrounds, an effect that confirms the patterns of global gene expression we observed in Figure 5 using an independent analysis tool. In contrast, the female data set showed only a few examples of clusters consistent with mitonuclear interactions (black squares in Figure 6).

### Cluster GO-enrichment analysis

To better understand which GO processes are associated with mitonuclear interactions, we performed a GO-enrichment analysis on each cluster in each sex. In females, 16/20 clusters contained GO terms that were significant ( $P < 0.05$ ) after

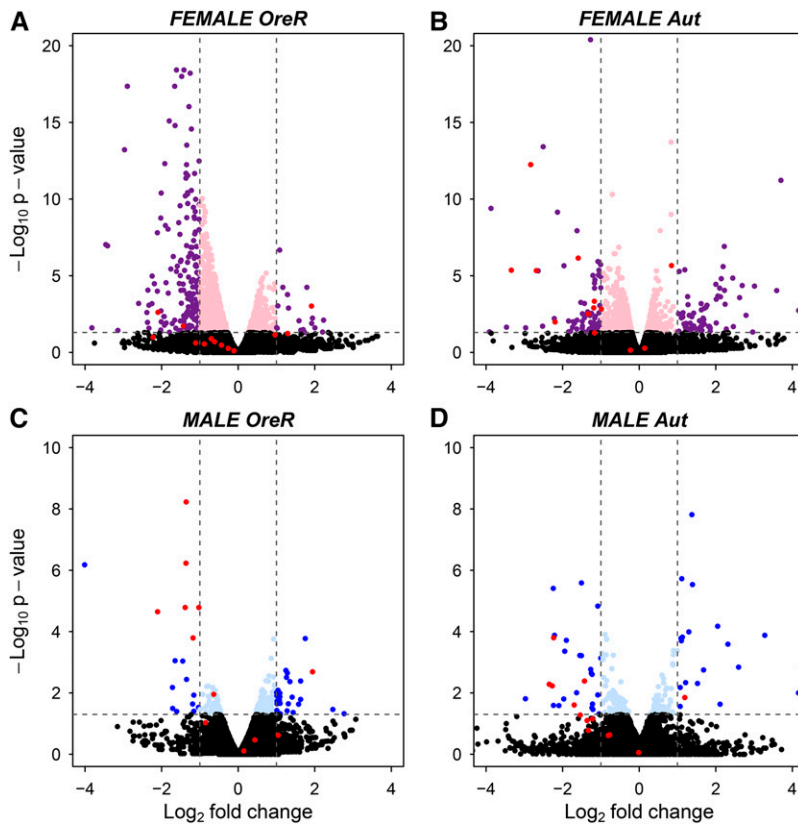


**Figure 3** Effects of mtDNA substitution on gene expression across nuclear backgrounds and sexes. Volcano plots describe the  $\log_2$ -fold change in expression of genes and their corresponding  $-\log_{10}$   $P$ -value, as determined by DESeq. Female genotypes are shown on the top panel: (A) *Oregon R* nDNA, and (B) *AutW132* nDNA. Males are shown on the bottom panel: (C) *Oregon R* nDNA, and (D) *AutW132* nDNA. Data in red are the mtDNA genes. There are nuclear background effects on mtDNA substitution and females generally showed more effects of mtDNA haplotype on nuclear gene expression. Horizontal dashed lines show  $P$ -value cut offs at equivalent  $P = 0.05$ . Vertical dashed lines show  $\pm 2 \times$  fold up- or downregulation of a gene due to alternative mtDNAs with values shown for *sil* mtDNA, relative to the *OregonR* mtDNA. Outliers are not shown and females have a different magnitude of variation on the ordinal scale than males. Note the consistent red datum in the top right section of each plot (*ND2* gene).

Bonferroni correction (Antonov *et al.* 2008), whereas only 13/20 clusters contained enriched terms in males. The full lists and significance of the GO terms are shown in Figure S8 (females) and Figure S9 (males).

Clusters with clear mitonuclear effects in females were clusters 17 and 18 (Figure 6). The most significantly enriched GO terms in these clusters were generally related to mitochondrial-ribosomal and protein translational processes (see clusters 17 and 18 in Figure S8).

### edgeR statistical analyses

The clustering approach provided qualitative support for an excess of mitonuclear interactions in males, and a larger proportion of mtDNA effects in females. To formally test the effects of mtDNA, nuclear, and mitonuclear variation, we conducted a DE analysis using *edgeR* (Robinson *et al.* 2010) in each sex separately. We conducted separate tests in males and females because the RNA-seq libraries have inherent differences in dispersion (biological coefficients of variation) between sexes. Stratifying the analyses by sex ensured that we made comparisons of genetic effects using appropriate dispersion estimates without conflating the DE estimates.

Figure 7, A and B, describes the distributions of significantly differentially expressed genes ( $P < 0.05$ ) in a sex-biased expression context. The plotted data are the mean expression values across all RNA-seq libraries in each sex. Significantly, DE genes corresponding to the three forms of genetic variation (mtDNA, nuclear, and mitonuclear) are

highlighted as black, purple, and green data, respectively. In females (Figure 7A), there was a large overlap between DE genes from all three sources of genetic manipulation but these significant genes were not enriched in female- or male-biased genes. Likewise in males, the majority of genes significantly differentially expressed by nuclear type were found in both non-sex-biased regions of the distribution, along with male-limited regions that correspond with testes and sperm-related biological processes (Figure 1, Table 1). While we found a few genes in the male-limited region of the distribution that were DE by mtDNA variation, DE genes associated with mtDNA haplotype variation were not enriched in this region (Figure 7B).

Across sexes, there were magnitudinal differences in the numbers of genes differentially expressed by mtDNA, nuclear, and mtDNA  $\times$  nuclear variation (Figure 7C); females showed larger responses to mtDNA and mitonuclear interactions, whereas males demonstrated marginally greater numbers of nuclear DE genes. For mtDNA variation (*sil/OregonR*), females demonstrated upregulation of 70 genes, and 39 genes were upregulated in males. There were 621 downregulated genes in females and 26 in males. By far the largest source of DE was for nuclear genetic variation (*AutW132/OregonR*) in both females (1737 up, 1952 down) and males (1836 up, 2246 down). Far fewer genes were associated with mitonuclear interactions (contrast *sil; AutW132 vs. OregonR; OregonR*) and these included 1462 in females and 556 in males. Interestingly, males showed larger numbers of DE genes in the mitonuclear category than in the first-order



**Table 2 Genes intersected in both males and females and in both nuclear backgrounds in response to mtDNA substitution**

Gene name	Flybase ID	Location	Symbol	CG number
A $\cap$ B $\cap$ C $\cap$ D intersection				
CG11966	FBgn0037645	3R: 8,950,246..8,963,037 (-)	CG11966	CG11966
<b>Mitochondrial NADH-ubiquinone oxidoreductase chain 2</b>	<b>FBgn0013680</b>	<b>mitochondrion_genome:240..1,265 (+)</b>	<b>mt:ND2</b>	<b>CG34063</b>
<b>Mitochondrial ATPase subunit 6</b>	<b>FBgn0013672</b>	<b>mitochondrion_genome:4,062..4,736 (+)</b>	<b>mt:ATPase6</b>	<b>CG34073</b>
<b>Mitochondrial NADH-ubiquinone oxidoreductase chain 4L</b>	<b>FBgn0013683</b>	<b>mitochondrion_genome:9,545..9,835 (-)</b>	<b>mt:ND4L</b>	<b>CG34086</b>
Jonah 25Bi	FBgn0020906	2L: 4,954,279..4,955,144 (-)	Jon25Bi	CG8867
A $\cap$ B $\cap$ C intersection				
Cyp28d1	FBgn0031689	2L: 5,210,460..5,212,445 (+)	Cyp28d1	CG10833
—	FBgn0035300	3L: 1,971,638..1,974,285 (+)	CG1139	CG1139
—	FBgn0038068	3R: 12,636,540..12,637,976 (+)	CG11600	CG11600
—	FBgn0033774	2R: 12,762,113..12,763,825 (+)	CG12374	CG12374
Chemosensory protein B 38c	FBgn0032888	2L: 20,820,089..20,820,867 (-)	CheB38c	CG14405
Integrin $\beta$ <sub>v</sub> subunit	FBgn0010395	2L: 21,053,033..21,058,044 (+)	Itg $\beta$ <sub>v</sub>	CG1762
$\epsilon$ Trypsin	FBgn0010425	2R: 11,345,237..11,346,066 (-)	$\epsilon$ Try	CG18681
Bent	FBgn0005666	4: 724,400..776,474 (+)	Bt	CG32019
—	FBgn0032494	2L: 13,239,989..13,241,773 (+)	CG5945	CG5945
—	FBgn0046999	2R: 16,873,015..16,873,755 (+)	CG6429	CG6429
Esterase 6	FBgn0000592	3L: 12,188,818..12,190,705 (+)	Est-6	CG6917
Hemolectin	FBgn0029167	3L: 13,846,054..13,860,001 (+)	Hml	CG7002
Henna	FBgn0001208	3L: 7,760,453..7,763,166 (+)	Hn	CG7399
Immune-regulated catalase	FBgn0038465	3R: 17,002,875..17,007,208 (+)	Irc	CG8913
A $\cap$ B $\cap$ D intersection				
Phosphoenolpyruvate carboxykinase	FBgn0003067	2R: 18,536,767..18,539,416 (+)	Pepck	CG17725
Ugt36Bc	FBgn0040260	2L: 16,799,025..16,801,584 (+)	Ugt36Bc	CG17932
Cyp6d5	FBgn0038194	3R: 14,029,228..14,031,483 (+)	Cyp6d5	CG3050
—	FBgn0052023	3L: 8,803,602..8,804,182 (-)	CG32023	CG32023
Ankyrin 2	FBgn0261788	3L: 7,655,389..7,718,395 (-)	Ank2	CG42734 <sup>a</sup>
—	FBgn0053346	3R: 28,669,233..28,670,452 (+)	CG33346	CG33346
lectin-37Db	FBgn0053533	2L: 19,419,075..19,419,767 (+)	lectin-37Db	CG33533
—	FBgn0053965	3L: 1,232,882..1,234,015 (+)	CG33965	CG33965
—	FBgn0085256	2R: 11,248,126..11,248,610 (+)	CG34227	CG34227
—	FBgn0038820	3R: 20,676,224..20,677,351 (-)	CG4000	CG4000
—	FBgn0039474	3R: 27,020,238..27,021,378 (-)	CG6283	CG6283
—	FBgn0037936	3R: 11,688,381..11,690,051 (-)	CG6908	CG6908
—	FBgn0039670	3R: 29,587,237..29,588,104 (-)	CG7567	CG7567
—	FBgn0039687	3R: 29,724,159..29,724,950 (-)	CG7593	CG7593
B $\cap$ C $\cap$ D intersection				
PGRP-SC2	FBgn0043575	2R: 8,716,950..8,717,695 (+)	PGRP-SC2	CG14745
PGRP-SC1a	FBgn0043576	2R: 8,709,733..8,710,320 (+)	PGRP-SC1a	CG14746
<b>Mitochondrial NADH-ubiquinone oxidoreductase chain 3</b>	<b>FBgn0013681</b>	<b>mitochondrion_genome: 5,608..5,961 (+)</b>	<b>mt:ND3</b>	<b>CG34076</b>
<b>Mitochondrial cytochrome b</b>	<b>FBgn0013678</b>	<b>mitochondrion_genome: 10,499..11,635 (+)</b>	<b>mt:Cyt-b</b>	<b>CG34090</b>
<b>Mitochondrial NADH-ubiquinone oxidoreductase chain 1</b>	<b>FBgn0013679</b>	<b>mitochondrion_genome: 11,721..12,659 (-)</b>	<b>mt:ND1</b>	<b>CG34092</b>

The genes required an unadjusted  $P$ -value  $\leq 0.05$  to be included in the analysis. The four-genotype intersection along with three three-way intersections are shown: (A) female *OregonR* background, (B) female *AutW132* background, (C) male *OregonR* background, and (D) male *AutW132* backgrounds. There were no genes present in the A $\cap$ C $\cap$ D intersection. Genes in boldface font are mtDNA protein coding genes.

<sup>a</sup> CG42734 overlaps with two additional computed genes (CGs): CG44195 and CG32373.

mtDNA category, consistent with the patterns we observed in the clustering analysis (see above).

To determine if genes behaved consistently across the sexes in response to genetic manipulation, we intersected those genes that were significantly differentially expressed ( $P < 0.05$ ) by mtDNA, nuclear, and mitonuclear variation from females and males. The between-sex intersections are shown in Figure 8. There were 26 genes that were consistently differentially expressed by mtDNA variation, 1426 genes differentially expressed by nDNA variation, and 124 that were

consistently differentially expressed by mitonuclear variation (Figure 8; gene identifications of the intersected genes can be found in Figure S10, Figure S11, and Figure S12). mtDNA genes are enriched in the intersected genes for mtDNA and nuclear variation, and *ATPase6*, *ND5*, and *ND6* demonstrate a consistent mitonuclear effect across the sexes. We found a large overlap between the consistently differentially expressed genes identified by DESeq (Table 2) and those identified by edgeR (Figure S10) as a consequence of mtDNA variation.



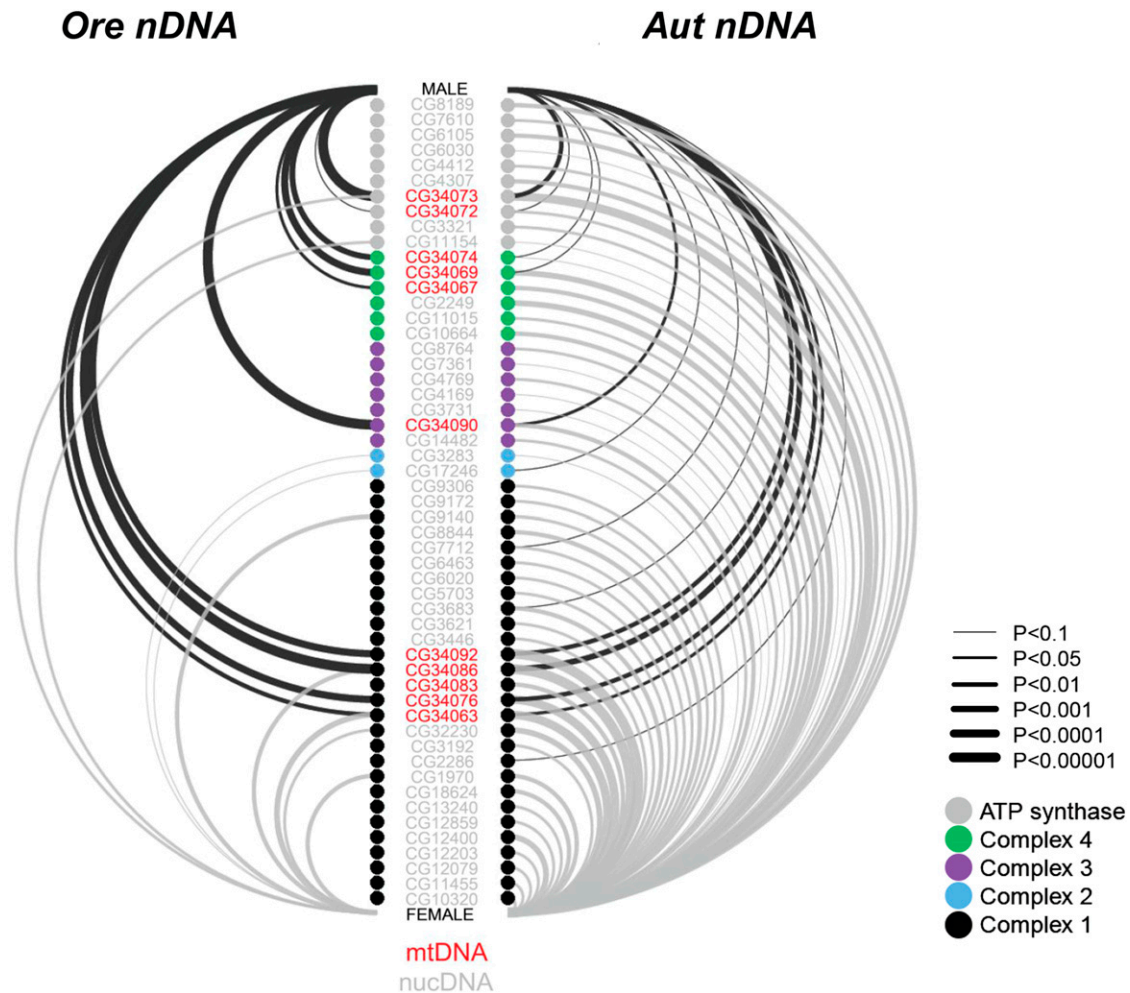


**Figure 4** OXPHOS-related genes are differentially expressed by mtDNA substitution. Arcdiagrams (Sanchez 2014) show the identities of OXPHOS genes whose expression levels are affected by mtDNA variation. Line thicknesses correspond with the significance level. Gene identifiers in red are those encoded by mtDNA. Male effects (black lines) and female effects (gray lines) are shown. Different OXPHOS complexes are differentiated by circle color: complex I, black; complex II, blue; complex III, purple; complex IV, green; ATP synthase (complex V), gray. The effects in the *OregonR* nuclear background are shown in the left plot; *AutW132*, on the right. The data shown are from the filtered data set. nucDNA, nDNA.

### Validating RNA-seq using qPCR

We used six nuclear genes that showed DE by nuclear variation and one internal control gene (*rp49*) to test whether the fold changes we measured using RNA-seq were correlated with qPCR. The methods and results can be found in File S1. The  $\log_2$ -fold change between *AutW132* and *Oregon R* in each mtDNA background was calculated for each gene in both sexes using the comparative threshold cycle ( $C_T$ ) method ( $2^{-\Delta\Delta CT}$ ) (Schmittgen and Livak 2008). We found a significant positive correlation between the  $\log_2$ -fold changes measured with RNA-seq and qPCR ( $r = +0.69$ ,  $t = 4.52$ , d.f. = 22,  $P = 0.00016$ ; Figure S13).

### Discussion

We tested for the effects of mtDNA, nuclear, and mitonuclear variation on gene expression variation and found both genotype- and sex-specific responses to all three forms of genetic

variation. Females showed overall stronger effects of genetic variation than males, and males showed little evidence of sex-limited expression of DE genes associated with mtDNA variation. mtDNA variation was most significantly associated with variation in mitochondrial OXPHOS gene expression and particularly those genes that are encoded by the mtDNA. In this panel of genotypes we found an overall opposing direction of mtDNA variation on global gene expression between the sexes, yet a conserved effect of mtDNA-encoded genes. Our findings are important to the *Drosophila* community, in which our reference strain, *OregonR*, has been widely adopted as a commonly used wild-type laboratory stock. Ongoing work in our laboratory aims to understand whether these effects are universal across multiple nuclear backgrounds, and not restricted to this particular nuclear *OregonR*-*AutW132* pair. We discuss our results in the context of OXPHOS protein organization, mtDNA-nDNA covariation, and the evolutionary significance of sex and genotype interactions.

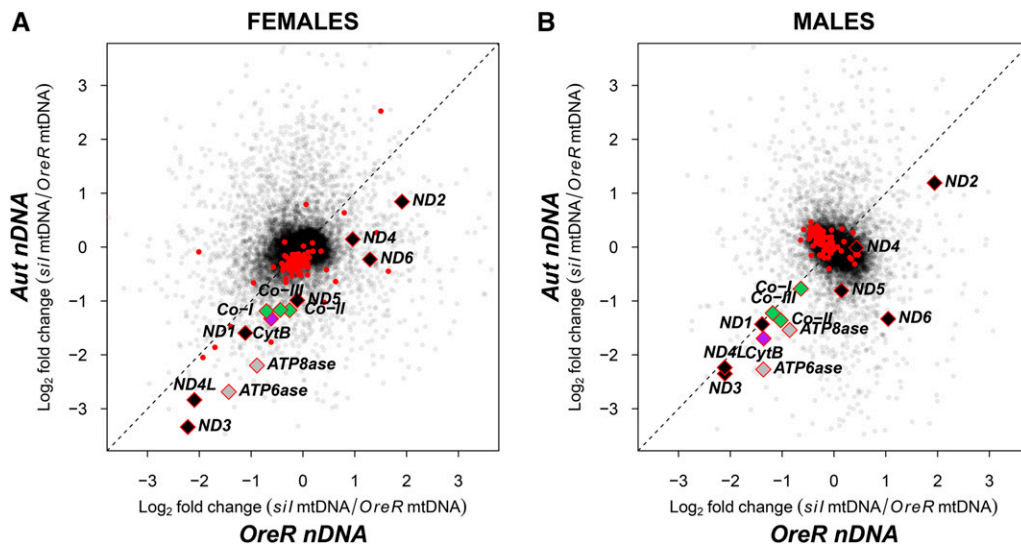


**Figure 5** Mitonuclear effects on gene expression differ between the sexes. Biplots of mtDNA effects on gene expression are shown for (A) females and (B) males. The effects of mtDNA substitution are reported as  $\log_2$ -fold changes in the *OregonR* and *AutW132* background on the abscissa and ordinal, respectively. mtDNA genes are labeled with their gene identifiers and show positive correlations between nuclear backgrounds in both sexes. Nuclear OXPHOS genes ( $n = 73$ ) are shown as red points. ND2 and ND3 genes were consistently ranked as the highest and lowest mtDNA genes, respectively. mtDNA genes are color coded by complex: complex I, black; complex III, purple; complex IV, green; ATP synthase, gray. Global gene correlations are reported in the main text.

### Mitochondrial gene expression and fitness

Gene expression variation in mtDNA and nuclear-encoded mitochondrial genes has been associated with a large number of human diseases, including cancer (Penta *et al.* 2001), neurodegenerative diseases (Schapira 1998; Swerdlow and Khan 2009), aging (Tońska *et al.* 2009), and type 2 diabetes mellitus (Mootha *et al.* 2003); however the exact mechanisms of action are poorly understood (Borowski *et al.* 2010). Early studies suggested the expression of OXPHOS genes in early development conditions the rate of electron transport enzyme activity throughout life in *Caenorhabditis elegans* (Dillin *et al.* 2002). More recently, knockdown of mitochondrial ribosomal proteins causes mitonuclear protein imbalance, reduced respiration, and activation of the mitochondrial UPR (Houtkooper *et al.* 2013). Paradoxically, this imbalance confers an overall positive, hormesis-like effect on life span and appears to be conserved between *C. elegans* and mammalian (mouse hepatocyte) cell lines. The regulation of mitochondrial genes is therefore important for organismal health, and transcript (or protein) imbalance between mitochondrial proteins may provide one arena for a cell to sense aberrant gene or protein function.

### mtDNA substitution affects mtDNA expression

We found expression levels of mtDNA genes to be among the most differentially expressed between mtDNA haplotypes. Importantly, these differences were not unidirectional across all genes. In all nuclear background  $\times$  sex combinations, the *sil* haplotype conferred upregulation of expression in some genes (e.g., ND2 gene), whereas genes from the same complex (complex I, e.g., ND3) were among the most downregulated genes as a consequence of mtDNA substitution. This

suggests that the relative abundance of transcripts is lower in *sil* haplotypes, however, there are exceptions to this rule (e.g., ND2). For mtDNA genes, we found a strong positive correlation between  $\log_2$ -fold changes in each nuclear background, suggesting that mtDNA genes behave similarly in different nuclear backgrounds and sexes. Importantly, there was a consistent rank order for the genes that were most up- and downregulated as a consequence of mtDNA substitution.

Mitochondrial haplotype variation has previously been shown to modify mtDNA copy number variation and mtDNA protein coding gene expression on a common nuclear background in *Drosophila* (Camus *et al.* 2015). In that study, the ND5 gene showed expression values consistent with phenotypic divergence, suggesting the mtDNA polymorphisms may behave as expression quantitative trait loci. The ND2 gene was not assayed in Camus *et al.*'s study due to its high A+T content, so comparisons between the present study and that study cannot be made. We show that mtDNA substitution can have a large impact on relative gene expression when large numbers of nucleotide polymorphisms are present in the contrasting genotypes (e.g.,  $\sim 103$  amino acid substitutions and 418 synonymous SNPs between *Oregon R* and *sil* haplotypes). The results from the current study show that the impact of mtDNA haplotypes on mtDNA gene expression may be an additive effect of the point mutations that differ between the compared haplotypes.

### Protein sequences or regulatory sequences?

Using the mitonuclear introgression model we specifically substituted alleles in the mtDNA coding region. We do not know the extent of mutations in the regulatory control region of the mtDNAs (D-loop), which is where transcription is initiated in *D. melanogaster* (Goddard and Wolstenholme

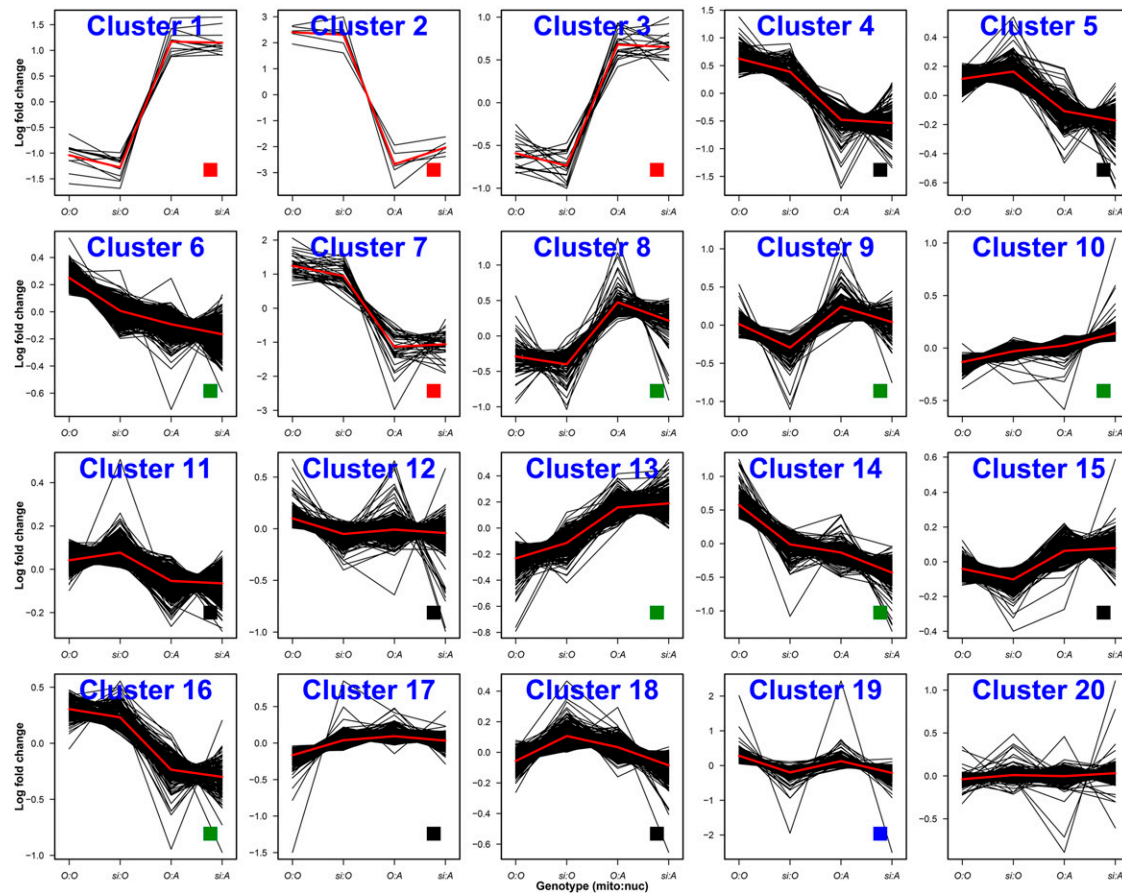


**Figure 6** Gene clusters demonstrating a spectrum of genetic effects in females. The abscissa shows the (mito; nuclear) genotype. The log-fold change is shown on the ordinal as determined by MBClusterSeq. The black lines outline individual zero-centered gene profiles across genotypes. The red line is the per-genotype mean value across all genes in the cluster. The cluster figure for males is shown in Figure S7. Colored squares show the main genetic effect captured by the cluster, as cartooned in Figure S1: red, nuclear effect; blue, mtDNA effect; green, nuclear + mtDNA effect; black, mtDNA  $\times$  nDNA interaction. *A*, *AutW132*; *O*, *OregonR*.

1978) and *D. simulans* (Goddard and Wolstenholme 1980). In both species, at least one (Clayton 1982) origin of replication occurs roughly in the center of the A+T-rich region (Goddard and Wolstenholme 1978; Wolstenholme 1992; Lewis *et al.* 1994; Torres *et al.* 2009). Our findings suggest that protein products of genes that assemble in a single complex (complex I) can have drastically different transcript abundance, and the mutations that segregate between *siI* and *OregonR* haplotypes alter expression in a gene-by-gene basis.

Complex I is one of the largest and most complicated enzymes in the eukaryotic cell (Vinothkumar *et al.* 2014), and its crystal structure has been resolved across a wide range of species, *e.g.*, *Escherichia coli* (Efremov and Sazanov 2011), *Thermus thermophilus* (Efremov *et al.* 2010), and *Bos taurus* (Vinothkumar *et al.* 2014). Among the consistent characteristics are the protein identifiers and their spatial organization within the membrane domain (Vinothkumar *et al.* 2014). One of the earliest genome-wide coexpression analyses provided good evidence in *Saccharomyces cerevisiae* that genes that physically interact or are present in the same metabolic pathway have similar expression levels (DeRisi *et al.* 1997). Our results show that a “healthy” fly can exhibit wide

variation in mtDNA transcripts from some complexes (*e.g.*, complex I), yet consistent coexpression patterns across other complexes (*e.g.*, complex IV and ATP synthase). Taken together, these results suggest some transcripts are more sensitive to genetic polymorphism than others, and that transcript variation within a protein complex may provide a useful trait to characterize the effects of mutations, and whether these effects are associated with deleterious phenotypes. Finally, the phenotypic effects on separate mitochondrial respiratory functions could help pinpoint whether complexes with tightly regulated transcripts perform better than those that have wide variation. If wide variation is deleterious, we would predict that complex I function, for example, would show more wide-ranging phenotypes between *siI* and *OregonR* haplotypes, than complex IV.

Why would *ND2* be massively upregulated and *ND3* massively downregulated as a result of *siI* mutations? In spite of their physical proximity in the mitochondrial inner membrane domain, we found those OXPHOS genes that were most sensitive to mtDNA variation are adjacent proteins (Vinothkumar *et al.* 2014). For example, Figure 5 shows that gene transcripts *ND3* and *ND4L* are closely grouped in the



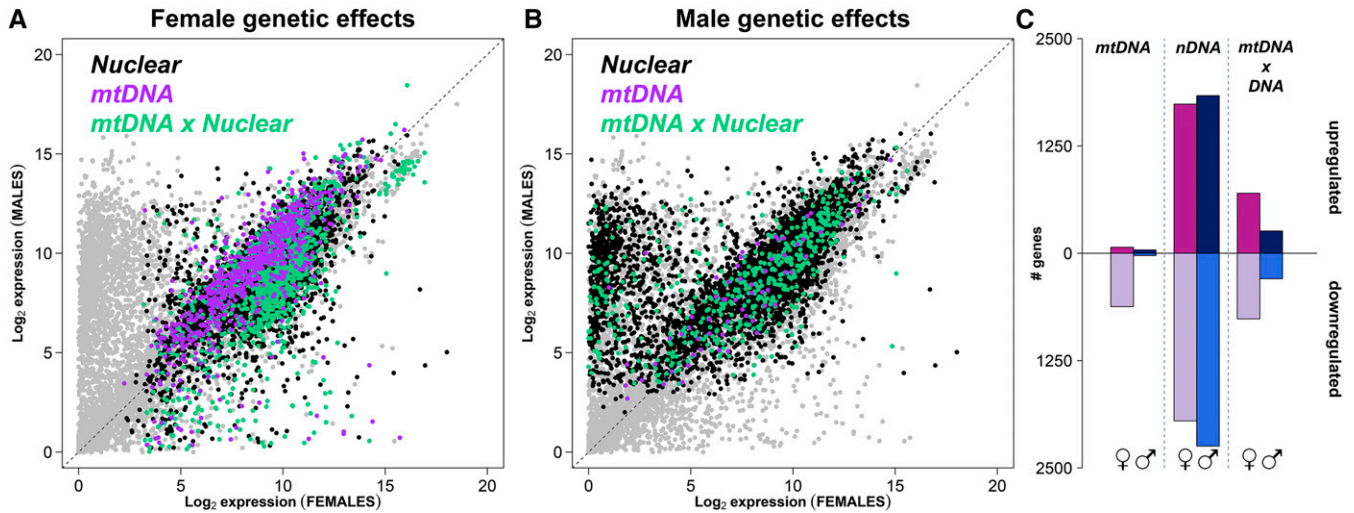


**Figure 7** The distribution of significant mtDNA, nDNA, and mitonuclear genotypes in expression space. Results of edgeR analyses on the complete data set are shown. Female expression is plotted on the abscissa, males on the ordinal. The position of differentially expressed genes by nuclear (black), mtDNA (purple), and mtDNA  $\times$  nDNA (green) variation are shown for (A) females and (B) males. The absolute numbers of significant genes in each category are described in bar plots in (C). Results for each category are divided into up- and downregulated genes. For each category females are shown leftmost, males rightmost.

plot. Likewise, *ND2* and *ND4* are consistently upregulated in both nuclear backgrounds and in both sexes. The patterns of expression are coextensive with the position of protein products; *ND3* and *ND4L*, and *ND2* and *ND4* are adjacent proteins in the membrane. Given that there are only seven mtDNA-encoded proteins in the membrane domain it is possible that this observation would be expected by chance, however it does suggest that conversion rates of transcript to protein may depend on the position of a protein in the membrane.

We have previously identified a number of SNPs that are different between the coding regions of *sil* and *OregonR* haplotypes and which have putative deleterious effects on protein function (Mossman *et al.* 2016). One of the private mutations to the *sil-OregonR* pair resides in the *ND2* gene and is two amino acids downstream of a putative deleterious amino acid polymorphism. Future work will aim to characterize whether this putative mutation is involved in the upregulation of the gene, possibly as a response to deleterious protein function; resulting in overall genetic robustness. Previous studies have shown that gene transcription responds to genetic mutation and may rescue phenotypes via a compensatory network (Kafri *et al.* 2005; Rossi *et al.* 2015). Moreover, during mammalian mtDNA transcription, polypeptides are theoretically transcribed in a 1:1 ratio because the polycistronic transcripts are fully transcribed from both mtDNA duplex strands (Gagliardi *et al.* 2004). In *Drosophila* mtDNA there are five different transcription initiation sites and transcript cleavage is signaled by the presence of cloverleaf structures of tRNAs (Ojala *et al.* 1981). There is considerable heterogeneity in mRNA expression between mtDNA genes within OXPHOS complexes, and these differences are largest in complex I (NADH dehydrogenase) (Torres *et al.* 2009). We also found NADH dehydrogenase to have the widest varia-

tion in  $\text{log}_2$ -fold change when comparisons were conducted within a gene (as a consequence of mtDNA variation). That is, mtDNA genetic variation was associated with differences in  $\text{log}_2$ -fold change. Taken together, these results suggest complex I gene expression shows wide variation (i) across genes within a complex and (ii) within genes as a consequence of mtDNA variation.

Following cleavage via endonucleases, polypeptide mRNAs are processed with a theoretical uniform abundance, which we did not observe. Given our haplotypes were from separate species, and those species have different control regions, with variable length and possibly SNP polymorphisms, it is possible that these regions alone are associated with the expression differences, with SNP variation having negligible effect. However, we favor the hypothesis that SNP variation does impact transcript levels, simply because a main effect of the regulatory (D-loop) region would presumably affect transcript levels in a more universal way, with little evidence of gene-specific expression patterns. Heterogeneity in transcript abundance across genes in *Drosophila* has been suggested to result from various post-transcriptional mechanisms including differential transcript stability and differences in the processing of mature transcripts (Torres *et al.* 2009). Our results suggest mtDNA variation can modify mtDNA gene transcriptional regulation and that complex I is particularly sensitive to mtDNA variation in this mtDNA haplotype pair (*OregonR* vs. *sil*).

#### Gene-by-gene interactions for transcription

mtDNA-encoded protein genes showed the most consistent patterns of DE identified using multiple analysis tools. Three mtDNA genes (*ND5*, *ND6*, and *ATPase6*; Figure S12) demonstrated a significant mitochondrial  $\times$  nuclear effect in both

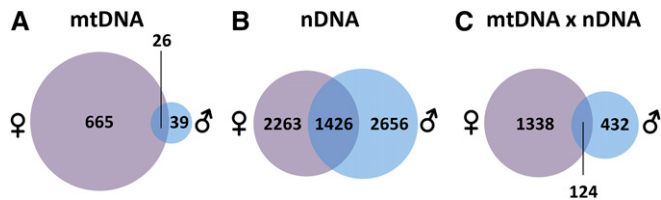


**Figure 8** Robust differentially expressed genes across (A) mtDNA, (B) nDNA, and (C) mtDNA  $\times$  nDNA categories. Venn diagrams describe the intersection of gene identifiers by sex in each category, as determined by DE analysis in edgeR on the complete data set. The area of the circles is relative to the number of genes within a category. Females are shown on the left, and males on the right of each diagram. Genes within the intersection between females and males are listed in Figure S10, Figure S11, and Figure S12 for each category, respectively.

sexes. That is, the effect of mtDNA substitution in one nuclear background was different from the effect in the other. As expected, nDNA variation was associated with DE in many genes in both males and females, however, we found females were generally more sensitive to mtDNA variation, particularly for OXPHOS complex genes. While males showed gene clusters consistent with mitonuclear effects, these were generally low magnitude differences and were not detected using DE analyses. We also found a larger effect in the *AutW132* nuclear background than in the *OregonR* nuclear background in females. Our gene lists (in Figure S10, Figure S11, and Figure S12) documenting the genes that were consistently differentially expressed across sexes are likely conservative estimates. On the other hand, they represent core sets of genes that are robustly differentially expressed across genetic backgrounds and sexes. Our clustering analyses showed clear evidence that many transcripts have gene-by-gene interaction patterns in males, yet mainly mtDNA effects in females; a pattern that was consistent across analysis tools. Interestingly, the nuclear genes involved in OXPHOS showed mitonuclear patterns in males, but no mitonuclear effects in females (red dots in Figure 5). Using an agnostic clustering approach, we identified sets of genes that showed similar expression patterns across genotypes and which were enriched for GO categories associated with mitochondrial function. It is now well established that genes in the same pathway share similar levels of expression (Stuart *et al.* 2003; Kafri *et al.* 2005) and we detected a strong signal that mitonuclear interaction gene clusters were enriched for processes involving translation and mitochondrial metabolism in both sexes. Moreover, the mtDNA OXPHOS genes tended to cluster in complex-specific clusters and this effect was more noticeable in females than in males. Similar results have been observed in humans where genes from distinct OXPHOS complexes tend to cluster together (van Waveren and Moraes 2008).

#### **The female transcriptome is more sensitive to genetic variation**

Considering the global gene set, we found that females exhibit clear genotype-specific transcript profiles regardless of the gene set analyzed. In contrast, the MDS plots revealed males

are distinguishable by nuclear backgrounds across all genes, but the effects of mtDNA are only present in the most differentially expressed gene sets and mainly restricted to the *AutW132* nuclear background. This first suggests that mtDNA genes are among the most differentially expressed in males, and second, that mtDNA  $\times$  nDNA interactions are present in males, and these operate on a large subset of the complete gene set. These were generally smaller in magnitude than in females. This phenomenon may help explain why a greater number of mitonuclear interactions were observed in males via gene clustering and these made detection of first-order effects of mtDNA and nuclear variation more difficult as fewer genes achieved statistical significance with DE-analysis tools. Using a combination of DE analyses provides clearer evidence that male and female transcriptomes respond differently to mitonuclear variation, and suggests a much larger number of genes are sensitive to mitonuclear variation in males, even though these are not “significantly” differentially expressed.

#### **Retrograde signaling is more prevalent in females**

We found mtDNA substitution in females conferred large effects on nuclear genes, suggesting pervasive retrograde signaling (mtDNA-to-nDNA feedback) between the genomes, and a clear separation of genotypes based on transcript expression. The effects of mtDNA variation were less obvious in males and a significantly smaller number of nuclear genes responded to mtDNA variation. While we acknowledge that there could be inherent differences between the male and female RNA-seq libraries due to a block effect, we conducted the majority of analyses within a sex to minimize a block effect on analyses interpretation. The magnitude and direction of  $\log_2$ -fold change in mtDNA genes were similar across sexes, suggesting we were able to capture real biological signal for the most differentially expressed genes. Importantly, when correlations (Figure 5) were compared across sexes, our mitonuclear results demonstrate a clear sexual dimorphism, even though the within-sex effects were calculated with sex-specific dispersion parameters. Under a null hypothesis of no sex-specific mitonuclear effect, we would not expect the sexes to differ in the direction of effect for the global pattern of expression. Given that the majority of male transcripts did not respond significantly to first-order mtDNA variation, the global transcript negative correlation we observed between nuclear backgrounds may be a product of reduced signal of mtDNA effects. However, mtDNA genes did respond and the mtDNA effect, while small for the majority of the transcriptome, was in the opposite direction in females. Our results show that the sensitivity to detect first-order effects of mtDNA variation are hindered by mitonuclear interactions, and a clustering approach is more likely to capture interaction effects. One interesting question arises: is this evidence of sexual antagonism (Rice 1984) for gene expression?

Genes from both mtDNA and nDNA genomes can respond to selection in females. The female environment likely provides the only opportunity for mitonuclear expression to be



exposed to selection, even though genes spend, on average, half their lifetime in each sex. Under this scenario, it has been suggested that nuclear genes that interact with mtDNAs would benefit from being on the *X* chromosome because there is greater opportunity for cotransmission and therefore coadaptation with mtDNA (Rand *et al.* 2001; Wade and Goodnight 2006). In *Drosophila*, the *X* chromosome has been implicated in mitonuclear epistatic interactions (Rand *et al.* 2001; Montooth *et al.* 2010), providing an opportunity to reduce intraindividual genetic conflict (*sensu* Werren 2011). However, mitonuclear genes are underrepresented on the *X* chromosome in *Drosophila* (Rogell *et al.* 2014), a pattern that is consistent also across various mammals (Drown *et al.* 2012) and *C. elegans* (Dean *et al.* 2014). Further, nuclear-mitochondrial gene duplications, which could help mitigate sexual conflict, are rarely relocated to the *X* chromosome in *Drosophila* (Gallach *et al.* 2010). In contrast, birds do not show under- or overrepresentation of mitonuclear genes on the *Z* chromosome (in birds, males are the homogametic sex and genes on the *Z* chromosome were tested; Drown *et al.* 2012).

Alternative sexual conflict-based hypotheses have been proposed to explain these observations (Drown *et al.* 2012; Dean *et al.* 2014; Rogell *et al.* 2014). Our results suggest pervasive retrograde signaling occurs between mtDNA and nuclear genes, motivating that future investigations on mitonuclear coevolution should focus on key regions of the nuclear genome that harbor mitonuclear interacting genes, and not just canonical OXPHOS or mitochondrial genes encoded by nDNA. For example, do these nuclear loci demonstrate evidence of unique patterns of selection compared to closely linked loci? We identified two nuclear genes, *CG11966* and *Jonah 25Bi*, that show consistent evidence of retrograde signaling in all genotypes and in both sexes. These genes are sensitive to mtDNA polymorphism, yet are not OXPHOS genes. We have also described a gene list of mitonuclear genes that are attractive targets of such a study (Figure S12).

#### **mtDNA effects are not limited to males or male-limited genes**

The Frank and Hurst hypothesis (Frank and Hurst 1996)—that males are more sensitive to mtDNA substitution—has limited support in this study. We found the mtDNA protein coding genes to be enriched in the gene list that was differentially expressed by mtDNA variation, and this effect was consistent across nuclear backgrounds. We also found a similar effect in females. While these findings suggest males are not suffering *more* than females as a result of mtDNA substitution, the enrichment of mtDNA genes *per se* is some evidence that males are sensitive to exclusively OXPHOS genes (Figure 4). It is possible that the nucleotide substitutions between *sil* and *OregonR* do not manifest with sufficiently large effect sizes on globally expressed genes to be detected in males, as has been observed in other mtDNA-variation studies on gene expression (Innocenti *et al.* 2011). Moreover in Innocenti *et al.*'s study, the effects of mtDNA substitution in a

*w1118 D. melanogaster* background were enriched in male-limited genes. Their finding evidenced a sex-specific selective sieve, whereby mtDNA mutations that were not under selection in males (due to maternal inheritance) could principally manifest in male-limited tissue as males are at a genetic dead end for mtDNA evolution. To independently test for mtDNA-associated expression differences in sex-limited genes, we also conducted our investigation on whole flies, including all reproductive tissue. We acknowledge that whole fly analyses cannot resolve sex-biased expression that may be due to differences in tissue contributions. However, we wanted to make our analyses comparable to other whole organism gene expression studies in *Drosophila*. We found no differences in fecundity between the strains used in this study (see File S1, Figure S14, Table S2, Table S3), suggesting the rate of turnover of gametes, and hence reproductive tissue mass, was not significantly different between strains and was unlikely to bias gene expression values between genotypes. Pathological mtDNA mutations principally manifest in tissues with high ATP demand (reviewed in Stewart and Chinnery 2015). The tissue-specific pathological effects of mtDNA variants in humans is a good motivation for future work to specifically test gene expression differences in tissues with high ATP demand in fruit flies, such as neuronal tissue, or flight muscle.

We did not recapitulate the sex-specific selective sieve effect in our study, in spite of (i) significant numbers of genes that demonstrated sex-specific gene expression (Figure 1), and (ii) large amounts of nucleotide variation between our haplotypes (>100 amino acid substitutions, and >400 synonymous mtDNA polymorphisms). Instead, we found no enrichment for mtDNA effects in male-biased genes [in regions of the gene expression space associated with male-limited traits (*e.g.*, spermatogenesis and testes)]. We only considered a pairwise comparison of mtDNA variation, in contrast to Innocenti *et al.*'s five haplotypes, and hence do not have the same polymorphisms present in our experiment. However, it is possible that the *w1118* nuclear background used in Innocenti *et al.* (2011) is more sensitive to mtDNA variation than other nuclear backgrounds and these differences may manifest disproportionately in males. In the present study we found greater mtDNA sensitivity in the *AutW132* background, providing good evidence that nuclear background *per se* can alter the sensitivity of the transcriptome to mtDNA variation. A main take home message in the present study is that there are differences between nuclear backgrounds and these can modify the effects of mtDNA variation. Extensive evidence of mtDNA  $\times$  nDNA interactions on phenotypes (Mossman *et al.* 2016), including comparisons with the *w1118* background (Zhu *et al.* 2014), suggests mtDNA haplotype-associated phenotypes are not always general results across nuclear backgrounds. We are now assessing the effects of environment on mitonuclear interactions to test whether mitonuclear effects are influenced by environment (gene-by-gene-by-environment interactions), or whether genotypes are robust to environmental perturbation. Previous studies suggest environment can have a large and sometimes

unpredictable effect on mitonuclear interactions (Mossman *et al.* 2016), however, there are no studies quantifying this in *Drosophila* gene expression.

In summary, we found considerable variation in transcript expression as a result of mtDNA, nDNA, and mitonuclear substitution. Contrary to the Frank and Hurst hypothesis, we did not find enrichment of mtDNA effects targeting male-limited gene expression in males. However, we did find large sex differences in the effects of genetic manipulation. In general, females showed larger genetic effects on transcript abundance and female genotypes were distinguishable based on their global gene-expression patterns, inconsistent with the lower sensitivity in males. In males, the majority of transcripts demonstrated mitonuclear effects in clustering analyses. Although mtDNA genes were preferentially differentially expressed, we interpret this as evidence that both mtDNA and nDNA covariation are important for transcript expression in this genotype panel. Future work will identify: (i) if these effects are general over a larger suite of genotypes, and (ii) by what mechanisms of action do mtDNA haplotypes affect gene expression. For example, are the polymorphisms in genic regions of the mtDNA responsible, or is variation in the mtDNA regulatory region key to the observed expression patterns? Are these effects tissue specific? Our general findings suggest that mtDNA effects can vary between nuclear genetic backgrounds depending on the sex tested, and therefore therapeutic methods to overcome mitochondrial diseases in humans should consider mitonuclear covariation as potential sources of phenotypic variation and therapy outcomes.

## Acknowledgments

We thank Christoph Schorl for assistance in the processing of RNA sequencing libraries, and Mark Howison for demultiplexing the samples. Jason Wood provided scripting help and Leann Biancani provided assistance with fly husbandry. A.-M. Hernandez gave critical comments on the manuscript. This work was conducted using computational resources and services at the Center for Computation and Visualization, Brown University. This project was funded by National Institutes of Health grants R01 GM-067862 and AG-027849 to D.M.R.

Author contributions: J.G.T. prepared flies for the experiment. J.A.M. and J.G.T. extracted RNA and conducted RNA sequencing. J.A.M. conducted the quantitative PCR analyses, analyzed the data with input from N.L. and W.Z., and wrote the manuscript with comments from D.M.R.

## Literature Cited

Anders, S., and W. Huber, 2010 Differential expression analysis for sequence count data. *Genome Biol.* 11: 1–12.  
Anders, S., P. T. Pyl, and W. Huber, 2015 HTSeq—a Python framework to work with high-throughput sequencing data. *Bioinformatics* 31: 166–169.  
Antonov, A. V., 2011 BioProfiling.de: analytical web portal for high-throughput cell biology. *Nucleic Acids Res.* 39: 323–327.

Antonov, A. V., T. Schmidt, Y. Wang, and H. W. Mewes, 2008 ProfCom: a web tool for profiling the complex functionality of gene groups identified from high-throughput data. *Nucleic Acids Res.* 36: 347–351.  
Ayroles, J. F., M. A. Carbone, E. A. Stone, K. W. Jordan, R. F. Lyman *et al.*, 2009 Systems genetics of complex traits in *Drosophila melanogaster*. *Nat. Genet.* 41: 299–307.  
Benjamini, Y., and Y. Hochberg, 1995 Controlling the false discovery rate: a practical and powerful approach to multiple testing. *J. R. Stat. Soc. B* 57: 289–300.  
Bernes, S. M., C. Bacino, T. R. Prezant, M. A. Pearson, T. S. Wood *et al.*, 1993 Identical mitochondrial DNA deletion in mother with progressive external ophthalmoplegia and son with Pearson marrow-pancreas syndrome. *J. Pediatr.* 123: 598–602.  
Borowski, L. S., R. J. Szczesny, L. K. Brzezniak, and P. P. Stepien, 2010 RNA turnover in human mitochondria: more questions than answers? *Biochim Biophys Acta* 1797: 1066–1070.  
Bourgon, R., R. Gentleman, and W. Huber, 2010 Independent filtering increases detection power for high-throughput experiments. *Proc. Natl. Acad. Sci. USA* 107: 9546–9551.  
Camus, M. F., D. J. Clancy, and D. K. Dowling, 2012 Mitochondria, maternal inheritance, and male aging. *Curr. Biol.* 22: 1717–1721.  
Camus, M. F., J. B. Wolf, E. H. Morrow, and D. K. Dowling, 2015 Single nucleotides in the mtDNA sequence modify mitochondrial molecular function and are associated with sex-specific effects on fertility and aging. *Curr. Biol.* 25: 2717–2722.  
Casademont, J., A. Barrientos, F. Cardellach, A. Rotig, J. M. Grau *et al.*, 1994 Multiple deletions of mtDNA in 2 brothers with sideroblastic anemia and mitochondrial myopathy and in their asymptomatic mother. *Hum. Mol. Genet.* 3: 1945–1949.  
Clayton, D. A., 1982 Replication of animal mitochondrial DNA. *Cell* 28: 693–705.  
D'Elia, D., D. Catalano, F. Licciulli, A. Turi, G. Tripoli *et al.*, 2006 The MitoDrome database annotates and compares the OXPHOS nuclear genes of *Drosophila melanogaster*, *Drosophila pseudoobscura* and *Anopheles gambiae*. *Mitochondrion* 6: 252–257.  
Dean, R., F. Zimmer, and J. E. Mank, 2014 The potential role of sexual conflict and sexual selection in shaping the genomic distribution of mito-nuclear genes. *Genome Biol. Evol.* 6: 1096–1104.  
DeRisi, J. L., V. R. Iyer, and P. O. Brown, 1997 Exploring the metabolic and genetic control of gene expression on a genomic scale. *Science* 278: 680–686.  
Dillin, A., A.-L. Hsu, N. Arantes-Oliveira, J. Lehrer-Graiwer, H. Hsin *et al.*, 2002 Rates of behavior and aging specified by mitochondrial function during development. *Science* 298: 2398–2401.  
Dimauro, S., and G. Davidzon, 2005 Mitochondrial DNA and disease. *Ann. Med.* 37: 222–232.  
DiMauro, S., and E. A. Schon, 2003 Mechanisms of disease: mitochondrial respiratory-chain diseases. *N. Engl. J. Med.* 348: 2656–2668.  
Drown, D. M., K. M. Preuss, and M. J. Wade, 2012 Evidence of a paucity of genes that interact with the mitochondrion on the X in mammals. *Genome Biol. Evol.* 4: 875–880.  
Eden, E., R. Navon, I. Steinfeld, D. Lipson, and Z. Yakhini, 2009 GOrrilla: a tool for discovery and visualization of enriched GO terms in ranked gene lists. *BMC Bioinformatics* 10: 1–7.  
Efremov, R. G., and L. A. Sazanov, 2011 Structure of the membrane domain of respiratory complex I. *Nature* 476: 414–420.  
Efremov, R. G., R. Baradaran, and L. A. Sazanov, 2010 The architecture of respiratory complex I. *Nature* 465: 441–445.  
Frank, S. A., and L. D. Hurst, 1996 Mitochondria and male disease. *Nature* 383: 224.  
Friberg, U., and D. K. Dowling, 2008 No evidence of mitochondrial genetic variation for sperm competition within a population of *Drosophila melanogaster*. *J. Evol. Biol.* 21: 1798–1807.

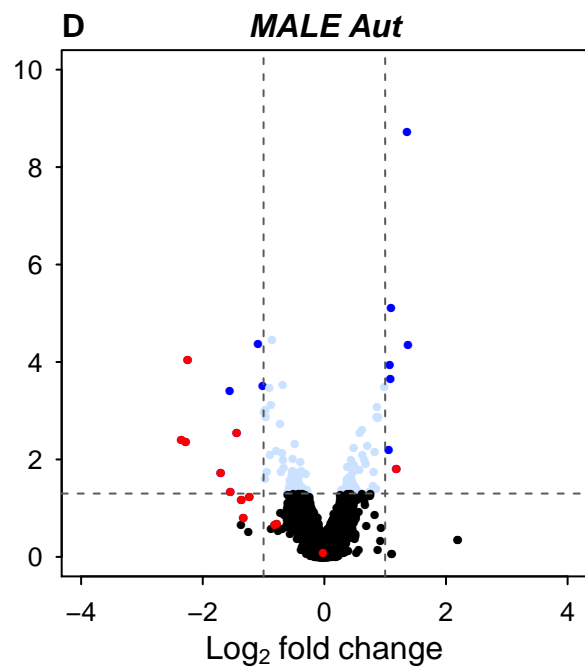
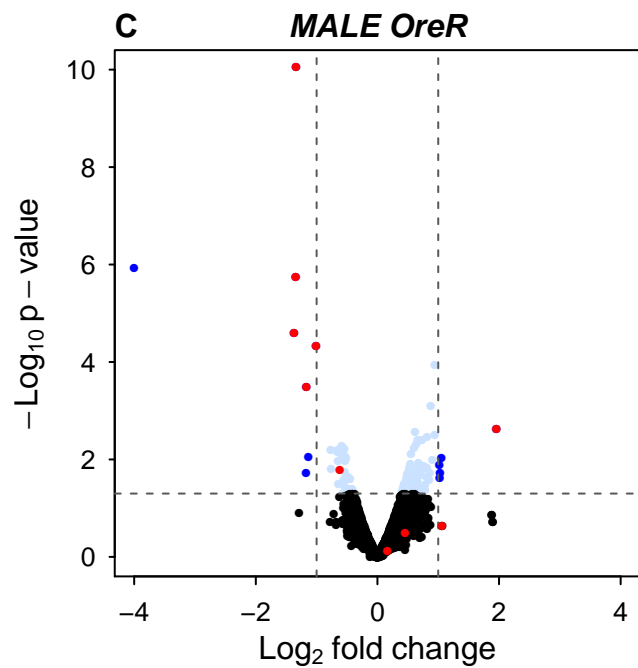
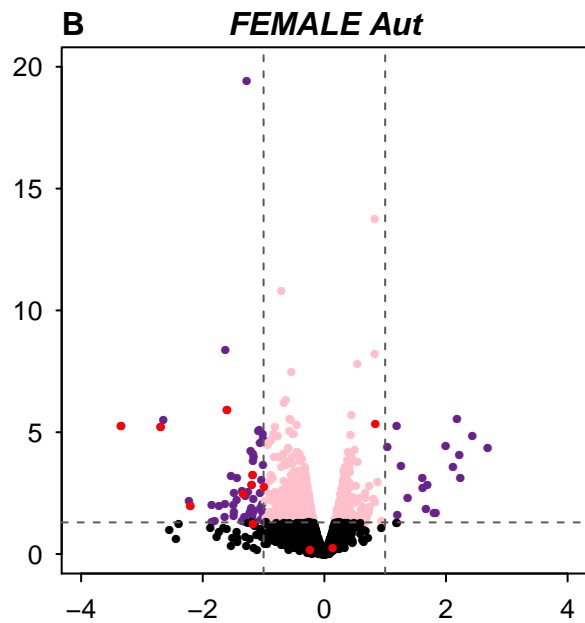
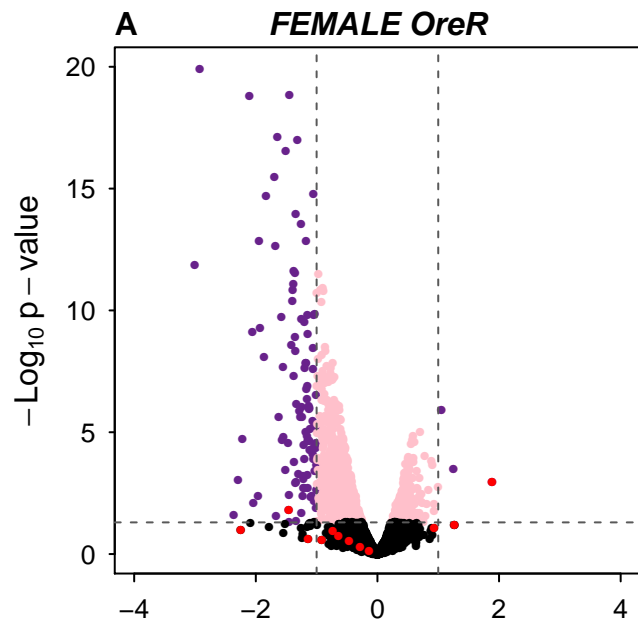
- Friedman, J. R., and J. Nunnari, 2014 Mitochondrial form and function. *Nature* 505: 335–343.
- Gagliardi, D., P. P. Stepien, R. J. Temperley, R. N. Lightowlers, and Z. M. A. Chrzanoska-Lightowlers, 2004 Messenger RNA stability in mitochondria: different means to an end. *Trends Genet.* 20: 260–267.
- Gallach, M., C. Chandrasekaran, and E. Betrán, 2010 Analyses of nuclearly encoded mitochondrial genes suggest gene duplication as a mechanism for resolving intralocus sexually antagonistic conflict in *Drosophila*. *Genome Biol. Evol.* 2: 835–850.
- Gemmell, N. J., V. J. Metcalf, and F. W. Allendorf, 2004 Mother's curse: the effect of mtDNA on individual fitness and population viability. *Trends Ecol. Evol.* 19: 238–244.
- Gibson, G., R. Riley-Berger, L. Harshman, A. Kopp, S. Vacha *et al.*, 2004 Extensive sex-specific nonadditivity of gene expression in *Drosophila melanogaster*. *Genetics* 167: 1791–1799.
- Giordano, C., L. Iommarini, L. Giordano, A. Maresca, A. Pisano *et al.*, 2014 Efficient mitochondrial biogenesis drives incomplete penetrance in Leber's hereditary optic neuropathy. *Brain* 137: 335–353.
- Goddard, J. M., and D. R. Wolstenholme, 1978 Origin and direction of replication in mitochondrial DNA molecules from *Drosophila melanogaster*. *Proc. Natl. Acad. Sci. USA* 75: 3886–3890.
- Goddard, J. M., and D. R. Wolstenholme, 1980 Origin and direction of replication in mitochondrial DNA molecules from the genus *Drosophila*. *Nucleic Acids Res.* 8: 741–757.
- Hoekstra, L. A., M. A. Siddiq, and K. L. Montooth, 2013 Pleiotropic effects of a mitochondrial-nuclear incompatibility depend upon the accelerating effect of temperature in *Drosophila*. *Genetics* 195: 1129–1139.
- Holmbeck, M. A., J. R. Donner, E. Villa-Cuesta, and D. M. Rand, 2015 A *Drosophila* model for mito-nuclear diseases generated by an incompatible interaction between tRNA and tRNA synthetase. *Dis. Model. Mech.* 8: 843–854.
- Houtkooper, R. H., L. Mouchiroud, D. Ryu, N. Moullan, E. Katsyuba *et al.*, 2013 Mitonuclear protein imbalance as a conserved longevity mechanism. *Nature* 497: 451–457.
- Huang, W., 2012 Epistasis dominates the genetic architecture of *Drosophila* quantitative traits. *Proc. Natl. Acad. Sci. USA* 109: 15553–15559.
- Huang, W., A. Massouras, Y. Inoue, J. Peiffer, M. Ramia *et al.*, 2014 Natural variation in genome architecture among 205 *Drosophila melanogaster* Genetic Reference Panel lines. *Genome Res.* 24: 1193–1208.
- Innocenti, P., E. H. Morrow, and D. K. Dowling, 2011 Experimental evidence supports a sex-specific selective sieve in mitochondrial genome evolution. *Science* 332: 845–848.
- Jacobs, H. T., and D. M. Turnbull, 2005 Nuclear genes and mitochondrial translation: a new class of genetic disease. *Trends Genet.* 21: 312–314.
- Kafri, R., A. Bar-Even, and Y. Pilpel, 2005 Transcription control reprogramming in genetic backup circuits. *Nat. Genet.* 37: 295–299.
- Lewis, D. L., C. L. Farr, A. L. Farquhar, and L. S. Kaguni, 1994 Sequence, organization, and evolution of the A+T region of *Drosophila melanogaster* mitochondrial DNA. *Mol. Biol. Evol.* 11: 523–538.
- Li, H., B. Handsaker, A. Wysoker, T. Fennell, J. Ruan *et al.*, 2009 The sequence alignment/map format and SAMtools. *Bioinformatics* 25: 2078–2079.
- Lin, M. T., and M. F. Beal, 2006 Mitochondrial dysfunction and oxidative stress in neurodegenerative diseases. *Nature* 443: 787–795.
- Mackay, T. F. C., S. Richards, E. A. Stone, A. Barbadilla, J. F. Ayroles *et al.*, 2012 The *Drosophila melanogaster* genetic reference panel. *Nature* 482: 173–178.
- Martin, W., and M. Muller, 1998 The hydrogen hypothesis for the first eukaryote. *Nature* 392: 37–41.
- Meiklejohn, C. D., M. A. Holmbeck, M. A. Siddiq, D. N. Abt, D. M. Rand *et al.*, 2013 An incompatibility between a mitochondrial tRNA and its nuclear-encoded tRNA synthetase compromises development and fitness in *Drosophila*. *PLoS Genet.* 9: e1003238.
- Montooth, K. L., C. D. Meiklejohn, D. N. Abt, and D. M. Rand, 2010 Mitochondrial-nuclear epistasis affects fitness within species but does not contribute to fixed incompatibilities between species of *Drosophila*. *Evolution* 64: 3364–3379.
- Mootha, V. K., C. M. Lindgren, K.-F. Eriksson, A. Subramanian, S. Sihag *et al.*, 2003 PGC-1[alpha]-responsive genes involved in oxidative phosphorylation are coordinately downregulated in human diabetes. *Nat. Genet.* 34: 267–273.
- Mossman, J. A., J. Slate, T. R. Birkhead, H. D. Moore, and A. A. Pacey, 2012 Mitochondrial haplotype does not influence sperm motility in a UK population of men. *Hum. Reprod.* 27: 641–651.
- Mossman, J. A., L. M. Biancani, C.-T. Zhu, and D. M. Rand, 2016 Mitonuclear epistasis for development time and its modification by diet in *Drosophila*. *Genetics* 203: 463–484.
- Ojala, D., J. Montoya, and G. Attardi, 1981 tRNA punctuation model of RNA processing in human mitochondria. *Nature* 290: 470–474.
- Penta, J. S., F. M. Johnson, J. T. Wachsman, and W. C. Copeland, 2001 Mitochondrial DNA in human malignancy. *Mutat. Res. Rev. Mutat. Res.* 488: 119–133.
- Pereira, L., J. Goncalves, R. Franco-Duarte, J. Silva, T. Rocha *et al.*, 2007 No evidence for an mtDNA role in sperm motility: data from complete sequencing of asthenozoospermic males. *Mol. Biol. Evol.* 24: 868–874.
- Pesole, G., J. F. Allen, N. Lane, W. Martin, D. M. Rand *et al.*, 2012 The neglected genome. *EMBO Rep.* 13: 473–474.
- Quiros, P. M., A. Mottis, and J. Auwerx, 2016 Mitonuclear communication in homeostasis and stress. *Nat. Rev. Mol. Cell Biol.* 17: 213–226.
- Rand, D. M., 2001 The units of selection on mitochondrial DNA. *Annu. Rev. Ecol. Syst.* 32: 415–448.
- Rand, D. M., A. G. Clark, and L. M. Kann, 2001 Sexually antagonistic cytonuclear fitness interactions in *Drosophila melanogaster*. *Genetics* 159: 173–187.
- Rice, W. R., 1984 Sex chromosomes and the evolution of sexual dimorphism. *Evolution* 38:735–742.
- Ritchie, M. E., B. Phipson, D. Wu, Y. Hu, C. W. Law *et al.*, 2015 limma powers differential expression analyses for RNA-sequencing and microarray studies. *Nucleic Acids Res.* 43: e47.
- Robinson, M. D., D. J. McCarthy, and G. K. Smyth, 2010 edgeR: a Bioconductor package for differential expression analysis of digital gene expression data. *Bioinformatics* 26: 139–140.
- Rogell, B., R. Dean, B. Lemos, and D. K. Dowling, 2014 Mitonuclear interactions as drivers of gene movement on and off the X-chromosome. *BMC Genomics* 15: 330.
- Rossi, A., Z. Kontarakis, C. Gerri, H. Nolte, S. Holper *et al.*, 2015 Genetic compensation induced by deleterious mutations but not gene knockdowns. *Nature* 524: 230–233.
- Roubertoux, P. L., F. Sluyter, M. Carlier, B. Marcet, F. Maarouf-Veray *et al.*, 2003 Mitochondrial DNA modifies cognition in interaction with the nuclear genome and age in mice. *Nat. Genet.* 35: 65–69.
- Ruiz-Pesini, E., A. C. Lapena, C. Diez-Sanchez, A. Perez-Martos, J. Montoya *et al.*, 2000 Human mtDNA haplogroups associated with high or reduced spermatozoa motility. *Am. J. Hum. Genet.* 67: 682–696.
- Sagan, L., 1967 On the origin of mitosing cells. *J. Theor. Biol.* 14: 225–274.

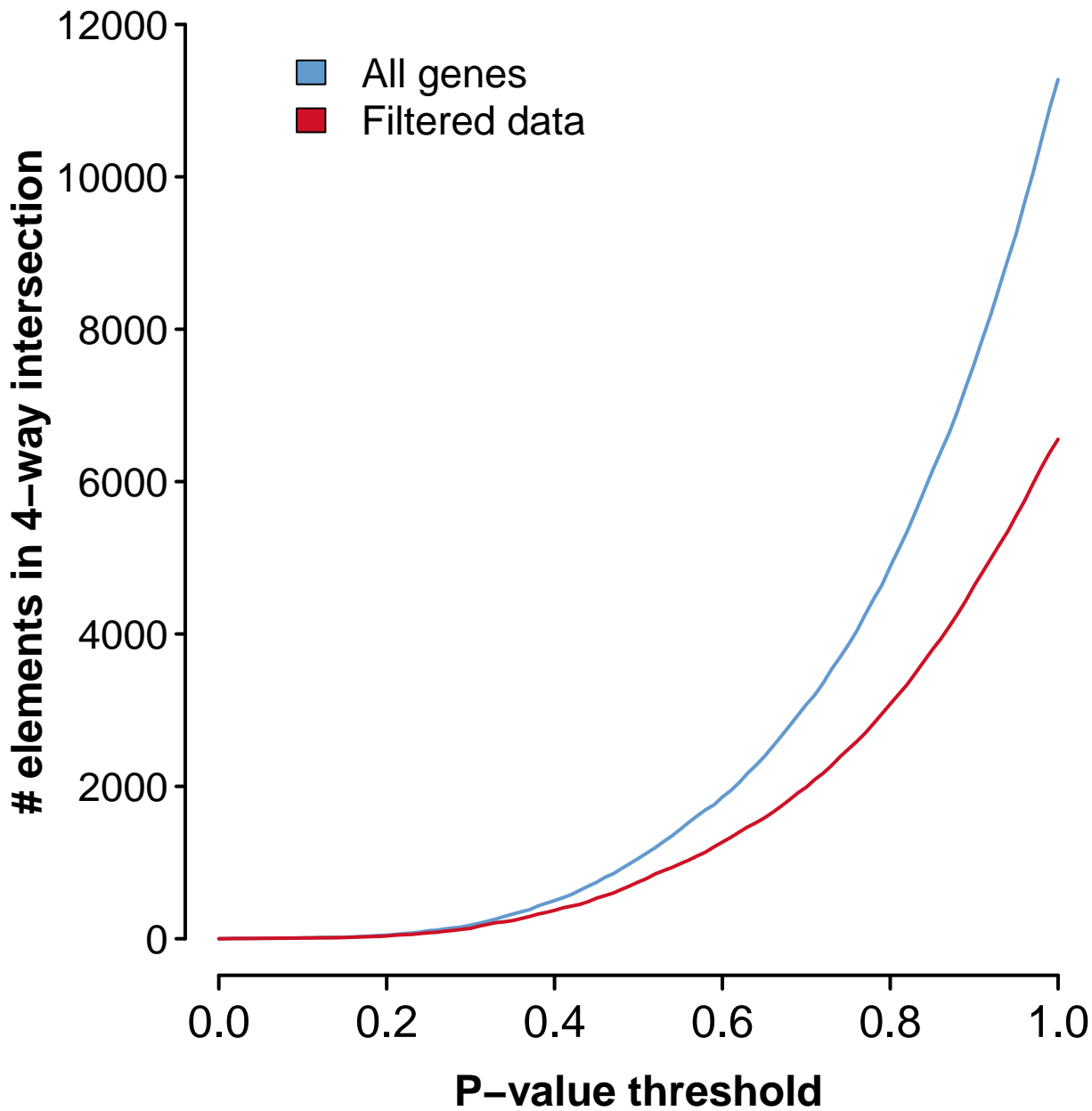
- Sanchez, G., 2014 Introduction to the R package arcDiagram. Available at: [http://gastonsanchez.com/software/arcDiagram\\_introduction.pdf](http://gastonsanchez.com/software/arcDiagram_introduction.pdf). Accessed September 8, 2016.
- Sardiello, M., F. Licciulli, D. Catalano, M. Attimonelli, and C. Caggese, 2003 MitoDrome: a database of *Drosophila melanogaster* nuclear genes encoding proteins targeted to the mitochondrion. *Nucleic Acids Res.* 31: 322–324.
- Schapira, A. H. V., 1998 Human complex I defects in neurodegenerative diseases. *Biochim Biophys Acta.* 1364: 261–270.
- Schmittgen, T. D., and K. J. Livak, 2008 Analyzing real-time PCR data by the comparative CT method. *Nat. Protoc.* 3: 1101–1108.
- Si, Y., P. Liu, P. Li, and T. P. Brutnell, 2014 Model-based clustering for RNA-seq data. *Bioinformatics* 30: 197–205.
- Smeitink, J., L. van den Heuvel, and S. DiMauro, 2001 The genetics and pathology of oxidative phosphorylation. *Nat. Rev. Genet.* 2: 342–352.
- Stewart, J. B., and P. F. Chinnery, 2015 The dynamics of mitochondrial DNA heteroplasmy: implications for human health and disease. *Nat. Rev. Genet.* 16: 530–542.
- Stuart, J. M., E. Segal, D. Koller, and S. K. Kim, 2003 A gene-coexpression network for global discovery of conserved genetic modules. *Science* 302: 249–255.
- Swerdlow, R. H., and S. M. Khan, 2009 The Alzheimer's disease mitochondrial cascade hypothesis: an update. *Exp. Neurol.* 218: 308–315.
- Taanman, J.-W., 1999 The mitochondrial genome: structure, transcription, translation and replication. *Biochim Biophys Acta.* 1410: 103–123.
- Tońska, K., A. Solyga, and E. Bartnik, 2009 Mitochondria and aging: innocent bystanders or guilty parties? *J. Appl. Genet.* 50: 55–62.
- Torres, T. T., M. Dolezal, C. Schlötterer, and B. Ottenwälder, 2009 Expression profiling of *Drosophila* mitochondrial genes via deep mRNA sequencing. *Nucleic Acids Res.* 37: 7509–7518.
- Trapnell, C., A. Roberts, L. Goff, G. Pertea, D. Kim *et al.*, 2012 Differential gene and transcript expression analysis of RNA-seq experiments with TopHat and Cufflinks. *Nat. Protoc.* 7: 562–578.
- Tripoli, G., D. D'Elia, P. Barsanti, and C. Caggese, 2005 Comparison of the oxidative phosphorylation (OXPHOS) nuclear genes in the genomes of *Drosophila melanogaster*, *Drosophila pseudoobscura* and *Anopheles gambiae*. *Genome Biol.* 6: 1–17.
- van Waveren, C., and C. T. Moraes, 2008 Transcriptional co-expression and co-regulation of genes coding for components of the oxidative phosphorylation system. *BMC Genomics* 9: 1–15.
- Villa-Cuesta, E., M. A. Holmbeck, and D. M. Rand, 2014 Rapamycin increases mitochondrial efficiency by mtDNA-dependent reprogramming of mitochondrial metabolism in *Drosophila*. *J. Cell Sci.* 127: 2282–2290.
- Vinothkumar, K. R., J. Zhu, and J. Hirst, 2014 Architecture of mammalian respiratory complex I. *Nature* 515: 80–84.
- Wade, M. J., and C. J. Goodnight, 2006 Cyto-nuclear epistasis: two-locus random genetic drift in hermaphroditic and dioecious species. *Evolution* 60: 643–659.
- Wallace, D. C., 1992 Diseases of the mitochondrial DNA. *Annu. Rev. Biochem.* 61: 1175–1212.
- Wallace, D. C., 1999 Mitochondrial diseases in man and mouse. *Science* 283: 1482–1488.
- Werren, J. H., 2011 Selfish genetic elements, genetic conflict, and evolutionary innovation. *Proc. Natl. Acad. Sci. USA* 108: 10863–10870.
- Wolstenholme, D. R., 1992 Animal mitochondrial DNA: structure and evolution, pp. 173–216 in *International Review of Cytology*, edited by R. W. David, and W. J. Kwang. Academic Press, San Diego.
- Wong, L. J. C., 2012 *Mitochondrial Disorders Caused by Nuclear Genes*. Springer, New York.
- Yee, W. K. W., K. L. Sutton, and D. K. Dowling, 2013 In vivo male fertility is affected by naturally occurring mitochondrial haplotypes. *Curr. Biol.* 23: 55–56.
- Zhu, C.-T., P. Ingelmo, and D. M. Rand, 2014 GxGxE for lifespan in *Drosophila*: mitochondrial, nuclear, and dietary interactions that modify longevity. *PLoS Genet.* 10: e1004354.

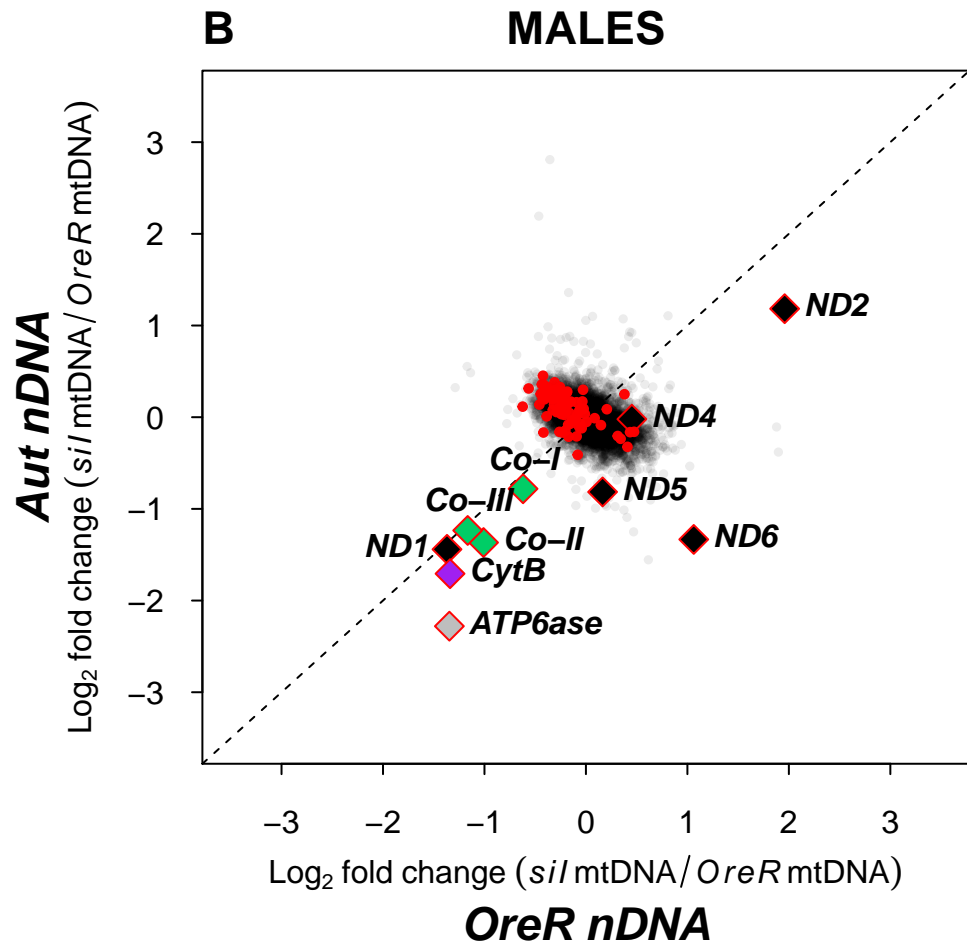
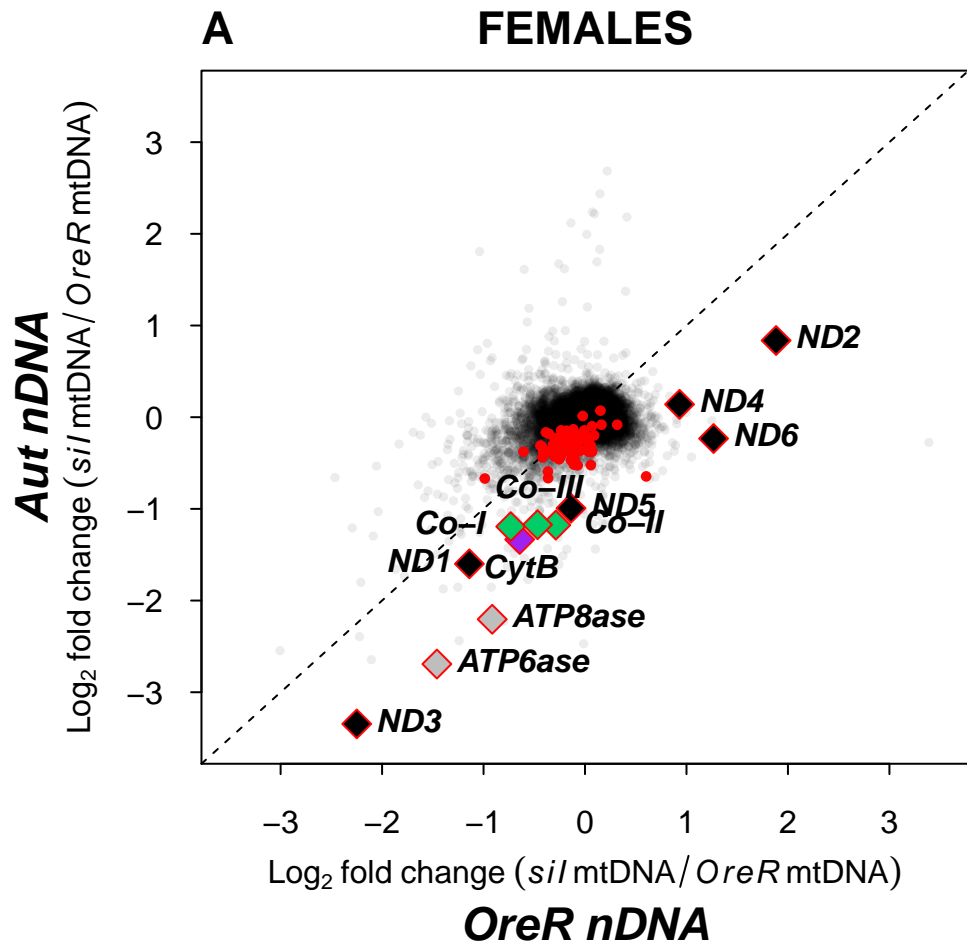
Communicating editor: J. A. Birchler



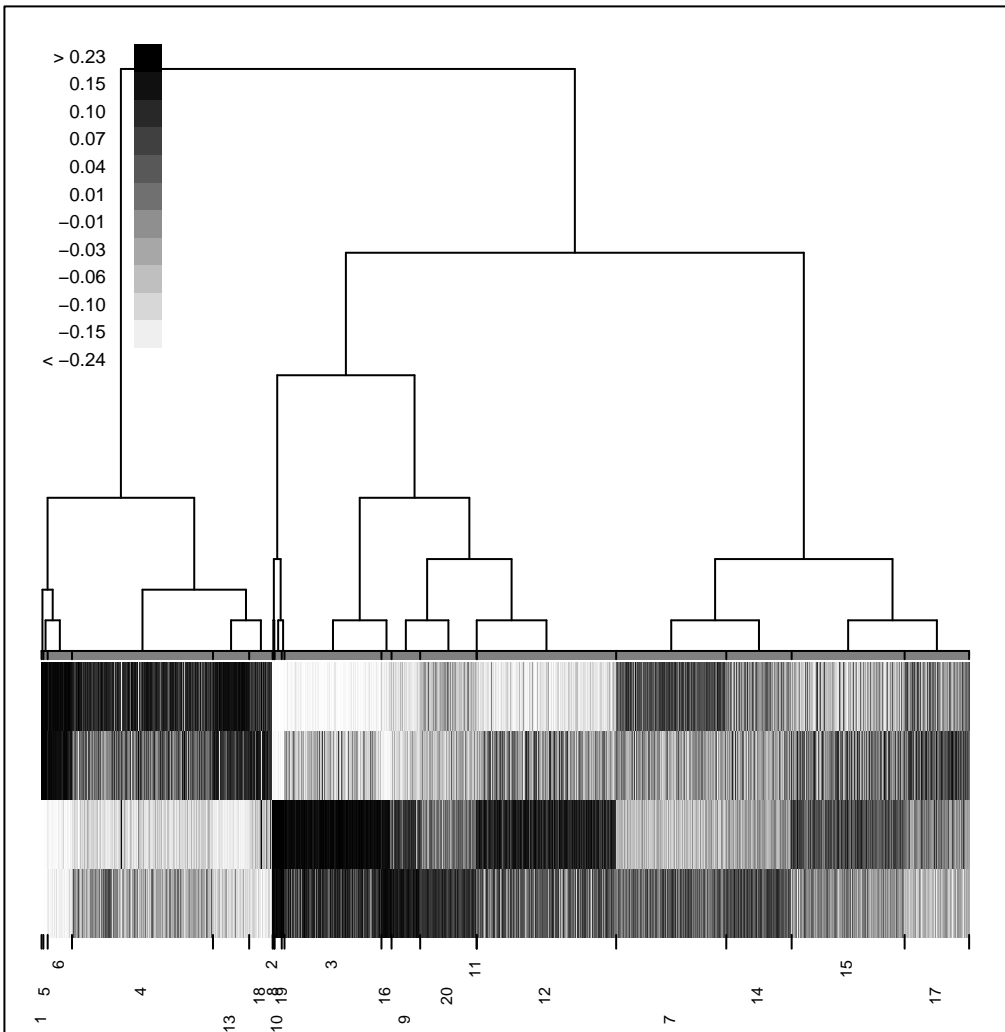




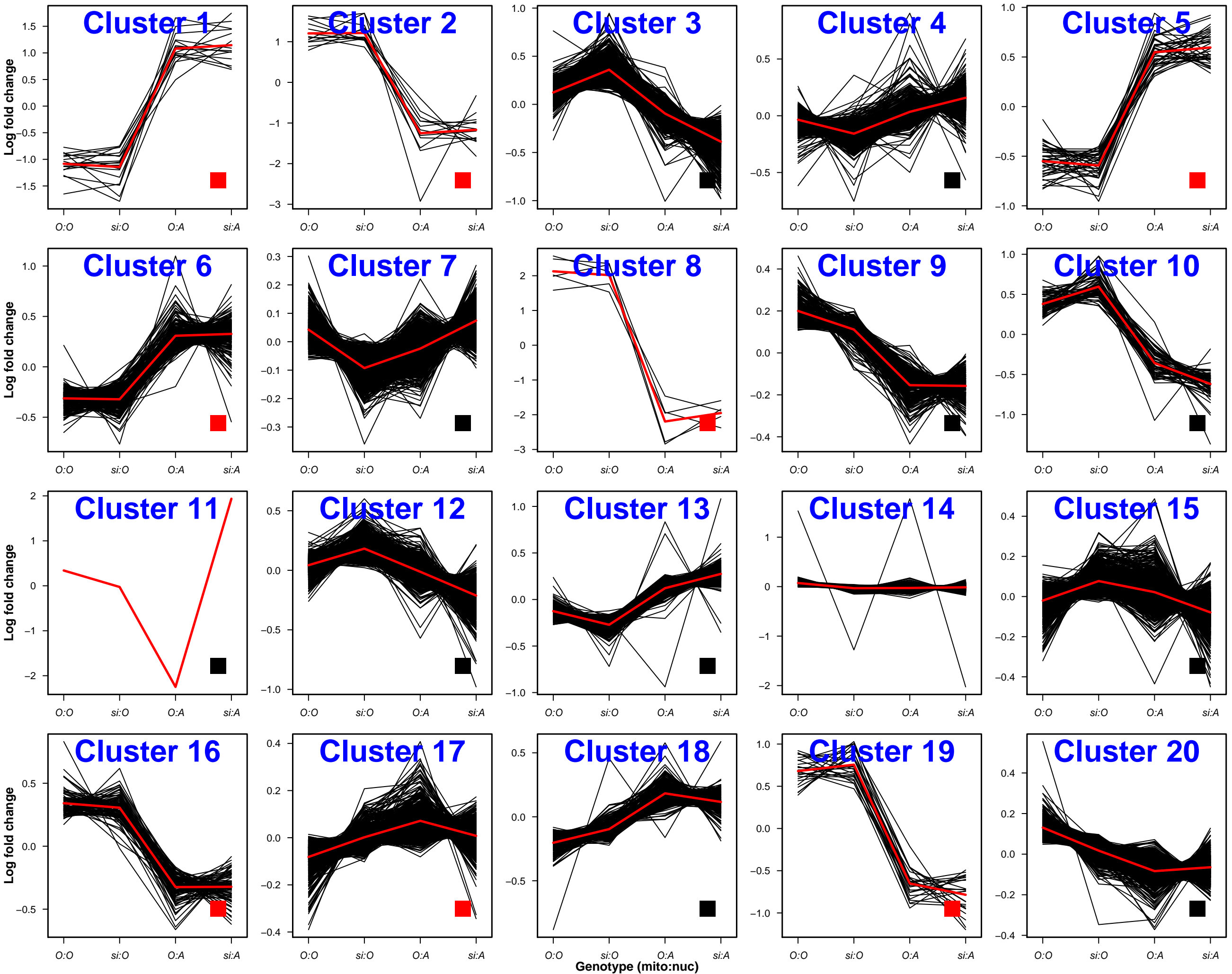








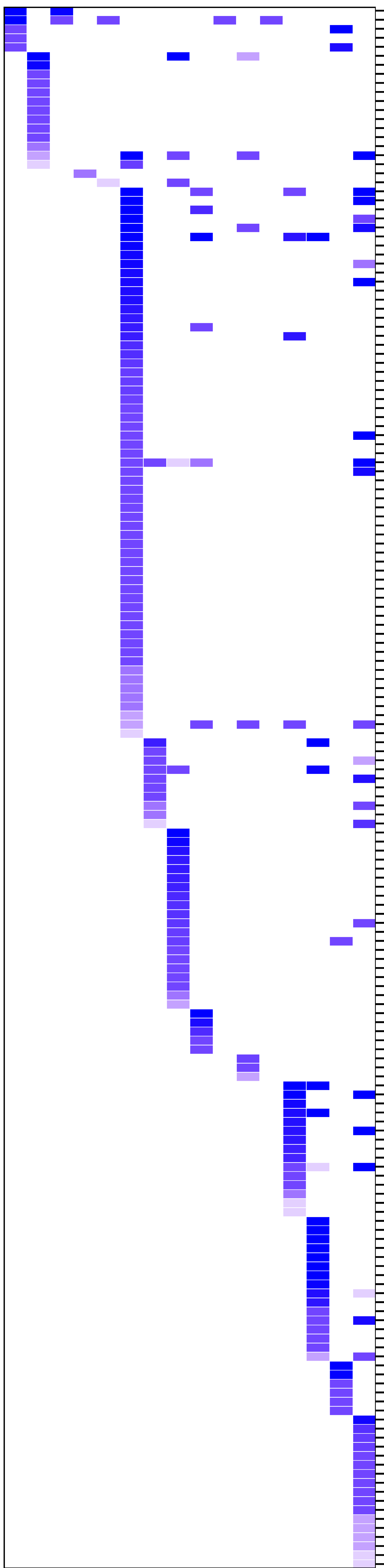






# GO enrichment FEMALES

p-value  
0.05  
0.04  
0.03  
0.02  
0.01  
0.00



- GO:0004252 SERINE-TYPE ENDOPEPTIDASE ACTIVITY
- GO:0006508 PROTEOLYSIS
- GO:0004497 MONOOXYGENASE ACTIVITY
- GO:0005576 EXTRACELLULAR REGION
- GO:0005792 MICROSOME
- GO:0005886 PLASMA MEMBRANE
- GO:0007427 EPITHELIAL CELL MIGRATION, OPEN TRACHEAL SYSTEM
- GO:0005887 INTEGRAL TO PLASMA MEMBRANE
- GO:0007432 SALIVARY GLAND BOUNDARY SPECIFICATION
- GO:0007498 MESODERM DEVELOPMENT
- GO:0007603 PHOTOTRANSDUCTION
- GO:0005811 PLATINUM ION
- GO:0018058 DEACTIVATION OF RHODOPSIN MEDIATED SIGNALING
- GO:0018199 AXON MIDLINE CHOICE POINT RECOGNITION
- GO:0016477 CELL MIGRATION
- GO:0006123 MITOCHONDRIAL ELECTRON TRANSPORT, CYTOCHROME C TO OXYGEN
- GO:0005515 PROTEIN BINDING
- GO:0007411 AXON GUIDANCE
- GO:0008152 METABOLIC PROCESS
- GO:0023034 INTRACELLULAR SIGNALING PATHWAY
- GO:0005634 NUCLEUS
- GO:0008270 ZINC ION BINDING
- GO:0003677 DNA BINDING
- GO:0005700 POLYTENE CHROMOSOME
- GO:0005732 CYTOPLASM
- GO:0007052 MITOTIC SPINDLE ORGANIZATION
- GO:0007173 MEIOSIS
- GO:00030178 NEGATIVE REGULATION OF WNT RECEPTOR SIGNALING PATHWAY
- GO:0048477 OOGENESIS
- GO:0016251 GENERAL RNA POLYMERASE II TRANSCRIPTION FACTOR ACTIVITY
- GO:0003676 NUCLEIC ACID BINDING
- GO:0042023 DNA ENDOREPLICATION
- GO:0009987 CELLULAR PROCESS
- GO:0017148 NEGATIVE REGULATION OF TRANSLATION
- GO:0004386 HELICASE ACTIVITY
- GO:0003887 DNA-DIRECTED DNA POLYMERASE ACTIVITY
- GO:0000776 KINETOCHORE
- GO:0048666 NEURON DEVELOPMENT
- GO:0005819 SPINDLE
- GO:0005810 CENTROSOME
- GO:0005811 MITOTIC CELL CYCLE
- GO:0000633 CYTOPLASMIC mRNA PROCESSING BODY
- GO:0007062 SISTER CHROMATID COHESION
- GO:0007476 IMAGINAL DISC-DERIVED WING MORPHOGENESIS
- GO:0000082 G1/S TRANSITION OF MITOTIC CELL CYCLE
- GO:0000910 CYTOKINESIS
- GO:0003714 TRANSCRIPTION COREPRESSOR ACTIVITY
- GO:0003729 MRNA BINDING
- GO:0003730 MRNA 3'-UTR BINDING
- GO:0004003 ATP-DEPENDENT DNA HELICASE ACTIVITY
- GO:0005524 ATP BINDING
- GO:0005622 INTRACELLULAR
- GO:0005828 KINETOCHORE MICROTUBULE
- GO:0005839 PROTEASOME REGULATORY PARTICLE
- GO:0005877 KINESIN COMPLEX
- GO:0006338 CHROMATIN REMODELING
- GO:0006339 UBIQUITIN-DEPENDENT PROTEIN CATABOLIC PROCESS
- GO:0006911 PHAGOCYTOSIS, ENGLUFMENT
- GO:0007049 CELL CYCLE
- GO:0007067 MITOSIS
- GO:0007094 MITOTIC CELL CYCLE SPINDLE ASSEMBLY CHECKPOINT
- GO:0007265 RAS PROTEIN SIGNAL TRANSDUCTION
- GO:0007307 EGGSHLL CHORION GENE AMPLIFICATION
- GO:0007465 R7 CELL FATE COMMITMENT
- GO:0008017 MICROTUBULE BINDING
- GO:0008586 IMAGINAL DISC-DERIVED WING VEIN MORPHOGENESIS
- GO:0016055 WNT RECEPTOR SIGNALING PATHWAY
- GO:0016563 TRANSCRIPTION ACTIVATOR ACTIVITY
- GO:0035019 SOMATIC STEM CELL MAINTENANCE
- GO:0035069 BRACHYDACTYL COMPLEX
- GO:0045893 NEGATIVE REGULATION OF SMOOTHENED SIGNALING PATHWAY
- GO:0045893 POSITIVE REGULATION OF TRANSCRIPTION, DNA-DEPENDENT
- GO:0048813 DENDRITE MORPHOGENESIS
- GO:0004221 UBIQUITIN THIOLESTERASE ACTIVITY
- GO:0004842 UBIQUITIN-PROTEIN LIGASE ACTIVITY
- GO:0005912 ADHERENS JUNCTION
- GO:0006261 DNA-DEPENDENT DNA REPLICATION
- GO:0006367 TRANSCRIPTION INITIATION FROM RNA POLYMERASE II PROMOTER
- GO:0003682 CHROMATIN BINDING
- GO:0005875 MICROTUBULE ASSOCIATED COMPLEX
- GO:0042127 REGULATION OF CELL PROLIFERATION
- GO:0022625 CYTOSOLIC LARGE RIBOSOMAL SUBUNIT
- GO:0000165 MAP K CASCADE
- GO:0005525 GTP BINDING
- GO:0008886 LIPID PARTICLE
- GO:0006914 INTRACELLULAR PROTEIN TRANSPORT
- GO:0006914 AUTOPHAGY
- GO:0016192 VESICLE-MEDIATED TRANSPORT
- GO:0000381 REGULATION OF ALTERNATIVE MRNA SPLICING, VIA SPLICEOSOME
- GO:0005778 PEROXISOMAL MEMBRANE
- GO:0004004 ATP-DEPENDENT RNA HELICASE ACTIVITY
- GO:0005925 FOCAL ADHESION
- GO:0003954 NADH DEHYDROGENASE ACTIVITY
- GO:0005747 MITOCHONDRIAL RESPIRATORY CHAIN COMPLEX I
- GO:0008137 NADH DEHYDROGENASE (UBIQUINONE) ACTIVITY
- GO:0007016 CYTOSKELETAL ANCHORING AT PLASMA MEMBRANE
- GO:0045202 SYNAPSE
- GO:0045197 ESTABLISHMENT OR MAINTENANCE OF EPITHELIAL CELL APICAL/BASAL POLARITY
- GO:0005859 CYTOSKELETON
- GO:0007769 ACTIN BINDING
- GO:0045168 LUSOME
- GO:0008360 REGULATION OF CELL SHAPE
- GO:0005938 CELL CORTEX
- GO:0055085 TRANSMEMBRANE TRANSPORT
- GO:0006120 MITOCHONDRIAL ELECTRON TRANSPORT, NADH TO UBIQUINONE
- GO:0006754 ATP BIOSYNTHETIC PROCESS
- GO:0007155 CELL ADHESION
- GO:0007268 SYNAPTIC TRANSMISSION
- GO:0007391 DORSAL CLOSURE
- GO:0016323 BASOLATERAL PLASMA MEMBRANE
- GO:0016021 INTEGRAL TO MEMBRANE
- GO:0006260 DNA REPLICATION
- GO:0006270 DNA REPLICATION INITIATION
- GO:0016320 FEMALE MEIOSIS CHROMOSOME SEGREGATION
- GO:0006381 DNA REPAIR
- GO:0007088 REGULATION OF MITOSIS
- GO:0031625 UBIQUITIN PROTEIN LIGASE BINDING
- GO:0051276 CHROMOSOME ORGANIZATION
- GO:0000922 SPINDLE POLE
- GO:0005762 MITOCHONDRIAL LARGE RIBOSOMAL SUBUNIT
- GO:0071011 PRECATALYTIC SPLICEOSOME
- GO:0006974 RESPONSE TO DNA DAMAGE STIMULUS
- GO:0003735 STRUCTURAL CONSTITUENT OF RIBOSOME
- GO:0004298 THREONINE-TYPE ENDOPEPTIDASE ACTIVITY
- GO:0071013 CATALYTIC STEP 2 SPLICEOSOME
- GO:0005839 PROTEASOME CORE COMPLEX
- GO:0005076 PROTEASOME COMPLEX
- GO:0004177 ENDOPEPTIDASE ACTIVITY
- GO:0000380 MRNA SPLICING VIA SPLICEOSOME
- GO:0031262 MITOTIC METAPHASE PLATE CONGRESSION
- GO:0031262 NDC80 COMPLEX
- GO:0019773 PROTEASOME CORE COMPLEX ALPHA-SUBUNIT COMPLEX
- GO:0007305 VITELLINE MEMBRANE FORMATION INVOLVED IN CHORION-CONTAINING EGGSHLL FORMATION
- GO:0051603 PROTEOLYSIS INVOLVED IN CELLULAR PROTEIN CATABOLIC PROCESS
- GO:0006412 TRANSLATION
- GO:0022627 CYTOSOLIC SMALL RIBOSOMAL SUBUNIT
- GO:0000022 MITOTIC SPINDLE ELONGATION
- GO:0005840 RIBOSOME
- GO:0005763 MITOCHONDRIAL SMALL RIBOSOMAL SUBUNIT
- GO:0000175 3'-5'-EXORIBONUCLEASE ACTIVITY
- GO:0000176 NUCLEAR EXOSOME (RNASE COMPLEX)
- GO:0000177 CYTOPLASMIC EXOSOME (RNASE COMPLEX)
- GO:0003293 RNA BINDING
- GO:0003293 RNA PROCESSING
- GO:0003890 DNA-DIRECTED RNA POLYMERASE ACTIVITY
- GO:0005681 SPLICEOSOMAL COMPLEX
- GO:0006413 TRANSLATIONAL INITIATION
- GO:0030532 SMALL NUCLEAR RIBONUCLEOPROTEIN COMPLEX
- GO:0042254 RIBOSOME BIOGENESIS
- GO:0003743 TRANSLATION INITIATION FACTOR ACTIVITY
- GO:0020037 HEME BINDING
- GO:0009055 ELECTRON CARRIER ACTIVITY
- GO:0005215 TRANSPORTER ACTIVITY
- GO:0005975 CARBOHYDRATE METABOLIC PROCESS
- GO:0043169 CATION BINDING
- GO:0055114 OXIDATION-REDUCTION PROCESS
- GO:0001660 NUCLEOTIDE BINDING
- GO:0032344 PROTEIN COMPLEX
- GO:0032344 RNA HELICASE ACTIVITY
- GO:0030036 ACTIN CYTOSKELETON ORGANIZATION
- GO:0003924 GTPASE ACTIVITY
- GO:0004674 PROTEIN SERINE/THREONINE KINASE ACTIVITY
- GO:0006468 PROTEIN PHOSPHORYLATION
- GO:0007015 ACTIN FILAMENT ORGANIZATION
- GO:0016197 ENDOSOMAL TRANSPORT
- GO:0042054 HISTONE METHYLTRANSFERASE ACTIVITY
- GO:0046974 HISTONE METHYLTRANSFERASE ACTIVITY (H3-K9 SPECIFIC)
- GO:0004672 PROTEIN KINASE ACTIVITY
- GO:0010883 REGULATION OF LIPID STORAGE
- GO:0016571 HISTONE METHYLATION
- GO:0046667 COMPOUND EYE RETINAL CELL PROGRAMMED CELL DEATH
- GO:0005705 POLYTENE CHROMOSOME INTERBAND
- GO:0008356 ASYMMETRIC CELL DIVISION

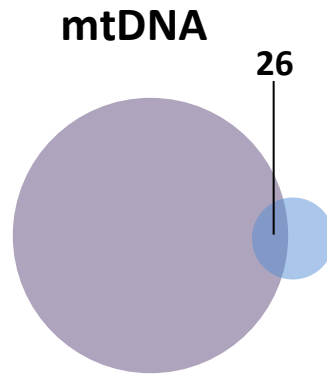
- Cluster 4
- Cluster 6
- Cluster 7
- Cluster 8
- Cluster 9
- Cluster 10
- Cluster 11
- Cluster 12
- Cluster 13
- Cluster 14
- Cluster 15
- Cluster 16
- Cluster 17
- Cluster 18
- Cluster 19
- Cluster 20







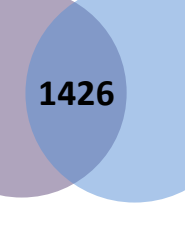
**Figure S10. Between sex gene intersections for mtDNA genes.** Those genes listed are consistently differentially expressed and intersected across the sexes.



Computed gene ID	Flybase ID	Gene ID
CG10011	FBgn0039590	<i>CG10011</i>
CG1165	FBgn0004430	<i>LysS</i>
CG11966	FBgn0037645	<i>CG11966</i>
CG15505	FBgn0039684	<i>Obp99d</i>
CG33256	FBgn0261565	<i>Lmpt</i>
CG3350	FBgn0039509	<i>bigmax</i>
CG34063	FBgn0013680	<i>mt:ND2</i>
CG34067	FBgn0013674	<i>mt:Col</i>
CG34069	FBgn0013675	<i>mt:Coll</i>
CG34072	FBgn0013673	<i>mt:ATPase8</i>
CG34073	FBgn0013672	<i>mt:ATPase6</i>
CG34074	FBgn0013676	<i>mt:ColIII</i>
CG34076	FBgn0013681	<i>mt:ND3</i>
CG34086	FBgn0013683	<i>mt:ND4L</i>
CG34090	FBgn0013678	<i>mt:Cyt-b</i>
CG34092	FBgn0013679	<i>mt:ND1</i>
CG4099	FBgn0014033	<i>Sr-CI</i>
CG42254	FBgn0259112	<i>CR42254</i>
CG4950	FBgn0036587	<i>CG4950</i>
CG5779	FBgn0283437	<i>PPO1</i>
CG7002	FBgn0029167	<i>Hml</i>
CG7106	FBgn0040099	<i>lectin-28C</i>
CG7171	FBgn0003961	<i>Uro</i>
CG8193	FBgn0033367	<i>PPO2</i>
CG8942	FBgn0259896	<i>NimC1</i>
CG9192	FBgn0035193	<i>CG9192</i>



Figure S11. Between sex gene intersections for nuclear genes. Those genes listed are consistently differentially expressed and intersected across the sexes.

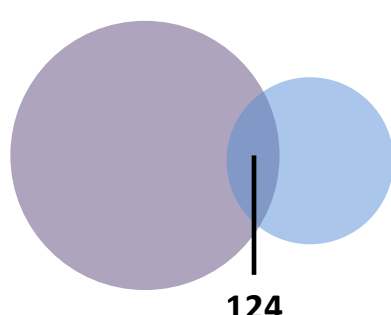


Computed GeneID	FbHyaseID	GeneID	Computed GeneID	FbHyaseID	GeneID	Computed GeneID	FbHyaseID	GeneID	Computed GeneID	FbHyaseID	GeneID
CG1000	Fbgm0039556	CG10001	CG14764	Fbgm0032336	CG14764	CG31973	Fbgm0051973	CG31973	CG5684	Fbgm0035948	CG5684
CG1001	Fbgm0039550	CG10011	CG14766	Fbgm0032338	CG14766	CG31979	Fbgm0051979	CG31979	CG5685	Fbgm0035956	CG5685
CG1002	Fbgm0039554	CG10021	CG14805	Fbgm0032341	CG14805	CG32006	Fbgm0052006	CG32006	CG5686	Fbgm0035964	CG5686
CG1003	Fbgm0039558	CG10031	CG14817	Fbgm0032343	CG14817	CG32023	Fbgm0052023	CG32023	CG5687	Fbgm0035972	CG5687
CG1004	Fbgm0039562	CG10041	CG14823	Fbgm0032345	CG14823	CG32025	Fbgm0052025	CG32025	CG5688	Fbgm0035980	CG5688
CG1005	Fbgm0039566	CG10051	CG14835	Fbgm0032347	CG14835	CG32030	Fbgm0052030	CG32030	CG5689	Fbgm0035988	CG5689
CG1006	Fbgm0039570	CG10061	CG14842	Fbgm0032349	CG14842	CG32037	Fbgm0052037	CG32037	CG5690	Fbgm0035996	CG5690
CG1007	Fbgm0039574	CG10071	CG14850	Fbgm0032351	CG14850	CG32040	Fbgm0052040	CG32040	CG5691	Fbgm0035994	CG5691
CG1008	Fbgm0039578	CG10081	CG14857	Fbgm0032353	CG14857	CG32056	Fbgm0052056	CG32056	CG5692	Fbgm0036002	CG5692
CG1009	Fbgm0039582	CG10091	CG14865	Fbgm0032355	CG14865	CG32096	Fbgm0052096	CG32096	CG5693	Fbgm0036010	CG5693
CG1010	Fbgm0039586	CG10101	CG14963	Fbgm0032359	CG14963	CG32107	Fbgm0052107	CG32107	CG5694	Fbgm0036018	CG5694
CG1011	Fbgm0039590	CG10111	CG14963	Fbgm0032359	CG14963	CG32112	Fbgm0052112	CG32112	CG5695	Fbgm0036026	CG5695
CG1012	Fbgm0039594	CG10121	CG14963	Fbgm0032359	CG14963	CG32121	Fbgm0052121	CG32121	CG5696	Fbgm0036034	CG5696
CG1013	Fbgm0039598	CG10131	CG14969	Fbgm0032363	CG14969	CG32152	Fbgm0052152	CG32152	CG5697	Fbgm0036042	CG5697
CG1014	Fbgm0039602	CG10141	CG15010	Fbgm0032367	CG15010	CG32165	Fbgm0052165	CG32165	CG5698	Fbgm0036050	CG5698
CG1015	Fbgm0039606	CG10151	CG15012	Fbgm0032369	CG15012	CG32177	Fbgm0052177	CG32177	CG5699	Fbgm0036058	CG5699
CG1016	Fbgm0039610	CG10161	CG15052	Fbgm0032373	CG15052	CG32230	Fbgm0052230	CG32230	CG5700	Fbgm0036066	CG5700
CG1017	Fbgm0039614	CG10171	CG15056	Fbgm0032377	CG15056	CG32243	Fbgm0052243	CG32243	CG5701	Fbgm0036074	CG5701
CG1018	Fbgm0039618	CG10181	CG15083	Fbgm0032381	CG15083	CG32266	Fbgm0052266	CG32266	CG5702	Fbgm0036082	CG5702
CG1019	Fbgm0039622	CG10191	CG15083	Fbgm0032381	CG15083	CG32280	Fbgm0052280	CG32280	CG5703	Fbgm0036090	CG5703
CG1020	Fbgm0039626	CG10201	CG15102	Fbgm0032385	CG15102	CG32282	Fbgm0052282	CG32282	CG5704	Fbgm0036098	CG5704
CG1021	Fbgm0039630	CG10211	CG15152	Fbgm0032389	CG15152	CG32289	Fbgm0052289	CG32289	CG5705	Fbgm0036106	CG5705
CG1022	Fbgm0039634	CG10221	CG15154	Fbgm0032393	CG15154	CG32302	Fbgm0052302	CG32302	CG5706	Fbgm0036114	CG5706
CG1023	Fbgm0039638	CG10231	CG15154	Fbgm0032393	CG15154	CG32317	Fbgm0052317	CG32317	CG5707	Fbgm0036122	CG5707
CG1024	Fbgm0039642	CG10241	CG15154	Fbgm0032393	CG15154	CG32324	Fbgm0052324	CG32324	CG5708	Fbgm0036130	CG5708
CG1025	Fbgm0039646	CG10251	CG15154	Fbgm0032393	CG15154	CG32326	Fbgm0052326	CG32326	CG5709	Fbgm0036138	CG5709
CG1026	Fbgm0039650	CG10261	CG15154	Fbgm0032393	CG15154	CG32339	Fbgm0052339	CG32339	CG5710	Fbgm0036146	CG5710
CG1027	Fbgm0039654	CG10271	CG15154	Fbgm0032393	CG15154	CG32342	Fbgm0052342	CG32342	CG5711	Fbgm0036154	CG5711
CG1028	Fbgm0039658	CG10281	CG15154	Fbgm0032393	CG15154	CG32348	Fbgm0052348	CG32348	CG5712	Fbgm0036162	CG5712
CG1029	Fbgm0039662	CG10291	CG15154	Fbgm0032393	CG15154	CG32348	Fbgm0052348	CG32348	CG5713	Fbgm0036170	CG5713
CG1030	Fbgm0039666	CG10301	CG15154	Fbgm0032393	CG15154	CG32348	Fbgm0052348	CG32348	CG5714	Fbgm0036178	CG5714
CG1031	Fbgm0039670	CG10311	CG15154	Fbgm0032393	CG15154	CG32348	Fbgm0052348	CG32348	CG5715	Fbgm0036186	CG5715
CG1032	Fbgm0039674	CG10321	CG15154	Fbgm0032393	CG15154	CG32348	Fbgm0052348	CG32348	CG5716	Fbgm0036194	CG5716
CG1033	Fbgm0039678	CG10331	CG15154	Fbgm0032393	CG15154	CG32348	Fbgm0052348	CG32348	CG5717	Fbgm0036202	CG5717
CG1034	Fbgm0039682	CG10341	CG15154	Fbgm0032393	CG15154	CG32348	Fbgm0052348	CG32348	CG5718	Fbgm0036210	CG5718
CG1035	Fbgm0039686	CG10351	CG15154	Fbgm0032393	CG15154	CG32348	Fbgm0052348	CG32348	CG5719	Fbgm0036218	CG5719
CG1036	Fbgm0039690	CG10361	CG15154	Fbgm0032393	CG15154	CG32348	Fbgm0052348	CG32348	CG5720	Fbgm0036226	CG5720
CG1037	Fbgm0039694	CG10371	CG15154	Fbgm0032393	CG15154	CG32348	Fbgm0052348	CG32348	CG5721	Fbgm0036234	CG5721
CG1038	Fbgm0039698	CG10381	CG15154	Fbgm0032393	CG15154	CG32348	Fbgm0052348	CG32348	CG5722	Fbgm0036242	CG5722
CG1039	Fbgm0039702	CG10391	CG15154	Fbgm0032393	CG15154	CG32348	Fbgm0052348	CG32348	CG5723	Fbgm0036250	CG5723
CG1040	Fbgm0039706	CG10401	CG15154	Fbgm0032393	CG15154	CG32348	Fbgm0052348	CG32348	CG5724	Fbgm0036258	CG5724
CG1041	Fbgm0039710	CG10411	CG15154	Fbgm0032393	CG15154	CG32348	Fbgm0052348	CG32348	CG5725	Fbgm0036266	CG5725
CG1042	Fbgm0039714	CG10421	CG15154	Fbgm0032393	CG15154	CG32348	Fbgm0052348	CG32348	CG5726	Fbgm0036274	CG5726
CG1043	Fbgm0039718	CG10431	CG15154	Fbgm0032393	CG15154	CG32348	Fbgm0052348	CG32348	CG5727	Fbgm0036282	CG5727
CG1044	Fbgm0039722	CG10441	CG15154	Fbgm0032393	CG15154	CG32348	Fbgm0052348	CG32348	CG5728	Fbgm0036290	CG5728
CG1045	Fbgm0039726	CG10451	CG15154	Fbgm0032393	CG15154	CG32348	Fbgm0052348	CG32348	CG5729	Fbgm0036298	CG5729
CG1046	Fbgm0039730	CG10461	CG15154	Fbgm0032393	CG15154	CG32348	Fbgm0052348	CG32348	CG5730	Fbgm0036306	CG5730
CG1047	Fbgm0039734	CG10471	CG15154	Fbgm0032393	CG15154	CG32348	Fbgm0052348	CG32348	CG5731	Fbgm0036314	CG5731
CG1048	Fbgm0039738	CG10481	CG15154	Fbgm0032393	CG15154	CG32348	Fbgm0052348	CG32348	CG5732	Fbgm0036322	CG5732
CG1049	Fbgm0039742	CG10491	CG15154	Fbgm0032393	CG15154	CG32348	Fbgm0052348	CG32348	CG5733	Fbgm0036330	CG5733
CG1050	Fbgm0039746	CG10501	CG15154	Fbgm0032393	CG15154	CG32348	Fbgm0052348	CG32348	CG5734	Fbgm0036338	CG5734
CG1051	Fbgm0039750	CG10511	CG15154	Fbgm0032393	CG15154	CG32348	Fbgm0052348	CG32348	CG5735	Fbgm0036346	CG5735
CG1052	Fbgm0039754	CG10521	CG15154	Fbgm0032393	CG15154	CG32348	Fbgm0052348	CG32348	CG5736	Fbgm0036354	CG5736
CG1053	Fbgm0039758	CG10531	CG15154	Fbgm0032393	CG15154	CG32348	Fbgm0052348	CG32348	CG5737	Fbgm0036362	CG5737
CG1054	Fbgm0039762	CG10541	CG15154	Fbgm0032393	CG15154	CG32348	Fbgm0052348	CG32348	CG5738	Fbgm0036370	CG5738
CG1055	Fbgm0039766	CG10551	CG15154	Fbgm0032393	CG15154	CG32348	Fbgm0052348	CG32348	CG5739	Fbgm0036378	CG5739
CG1056	Fbgm0039770	CG10561	CG15154	Fbgm0032393	CG15154	CG32348	Fbgm0052348	CG32348	CG5740	Fbgm0036386	CG5740
CG1057	Fbgm0039774	CG10571	CG15154	Fbgm0032393	CG15154	CG32348	Fbgm0052348	CG32348	CG5741	Fbgm0036394	CG5741
CG1058	Fbgm0039778	CG10581	CG15154	Fbgm0032393	CG15154	CG32348	Fbgm0052348	CG32348	CG5742	Fbgm0036402	CG5742
CG1059	Fbgm0039782	CG10591	CG15154	Fbgm0032393	CG15154	CG32348	Fbgm0052348	CG32348	CG5743	Fbgm0036410	CG5743
CG1060	Fbgm0039786	CG10601	CG15154	Fbgm0032393	CG15154	CG32348	Fbgm0052348	CG32348	CG5744	Fbgm0036418	CG5744
CG1061	Fbgm0039790	CG10611	CG15154	Fbgm0032393	CG15154	CG32348	Fbgm0052348	CG32348	CG5745	Fbgm0036426	CG5745
CG1062	Fbgm0039794	CG10621	CG15154	Fbgm0032393	CG15154	CG32348	Fbgm0052348	CG32348	CG5746	Fbgm0036434	CG5746
CG1063	Fbgm0039798	CG10631	CG15154	Fbgm0032393	CG15154	CG32348	Fbgm0052348	CG32348	CG5747	Fbgm0036442	CG5747
CG1064	Fbgm0039802	CG10641	CG15154	Fbgm0032393	CG15154	CG32348	Fbgm0052348	CG32348	CG5748	Fbgm0036450	CG5748
CG1065	Fbgm0039806	CG10651	CG15154	Fbgm0032393	CG15154	CG32348	Fbgm0052348	CG32348	CG5749	Fbgm0036458	CG5749
CG1066	Fbgm0039810	CG10661	CG15154	Fbgm0032393	CG15154	CG32348	Fbgm0052348	CG32348	CG5750	Fbgm0036466	CG5750
CG1067	Fbgm0039814	CG10671	CG15154	Fbgm0032393	CG15154	CG32348	Fbgm0052348	CG32348	CG5751	Fbgm0036474	CG5751
CG1068	Fbgm0039818	CG10681	CG15154	Fbgm0032393	CG15154	CG32348	Fbgm0052348	CG32348	CG5752	Fbgm0036482	CG5752
CG1069	Fbgm0039822	CG10691	CG15154	Fbgm0032393	CG15154	CG32348	Fbgm0052348	CG32348	CG5753	Fbgm0036490	CG5753
CG1070	Fbgm0039826	CG10701	CG15154	Fbgm0032393	CG15154	CG32348	Fbgm0052348	CG32348	CG5754	Fbgm0036498	CG5754
CG1071	Fbgm0039830	CG10711	CG15154	Fbgm0032393	CG15154	CG32348	Fbgm0052348	CG32348	CG5755	Fbgm0036506	CG5755
CG1072	Fbgm0039834	CG10721	CG15154	Fbgm0032393	CG15154	CG32348	Fbgm0052348	CG32348	CG5756	Fbgm0036514	CG5756
CG1073	Fbgm0039838	CG10731	CG15154	Fbgm0032393	CG15154	CG32348	Fbgm0052348	CG32348	CG5757	Fbgm0036522	CG5757
CG1074	Fbgm0039842	CG10741	CG15154	Fbgm0032393	CG15154	CG32348	Fbgm0052348	CG32348	CG5758	Fbgm0036530	CG5758
CG1075	Fbgm0039846	CG10751	CG15154	Fbgm0032393	CG15154	CG32348	Fbgm0052348	CG32348	CG5759	Fbgm0036538	CG5759
CG1076	Fbgm0039850	CG10761	CG15154	Fbgm0032393	CG15154	CG32348	Fbgm0052348	CG32348	CG5760	Fbgm0036546	CG5760
CG1077	Fbgm0039854	CG10771	CG15154	Fbgm0032393	CG15154	CG32348	Fbgm0052348	CG32348	CG5761	Fbgm0036554	CG5761
CG1078	Fbgm0039858	CG10781	CG15154	Fbgm0032393	CG15154	CG32348	Fbgm0052348	CG32348	CG5762	Fbgm0036562	CG5762
CG1079	Fbgm0039862	CG10791	CG15154	Fbgm0032393	CG15154	CG32348	Fbgm0052348	CG32348	CG5763	Fbgm0036570	CG5763
CG1080	Fbgm0039866	CG10801	CG15154	Fbgm0032393	CG15154	CG32348	Fbgm0052348	CG32348	CG5764	Fbgm0036578	CG5764
CG1081	Fbgm0039870	CG10811	CG15154	Fbgm0032393	CG15154	CG32348	Fbgm0052348	CG32348	CG5765	Fbgm0036586	CG5765
CG1082	Fbgm0039874	CG10821	CG15154	Fbgm0032393	CG15154	CG32348	Fbgm0052348	CG32348	CG5766	Fbgm0036594	



**Figure S12. Between sex gene intersections for mitonuclear genes.** Those genes listed are consistently differentially expressed and intersected across the sexes.

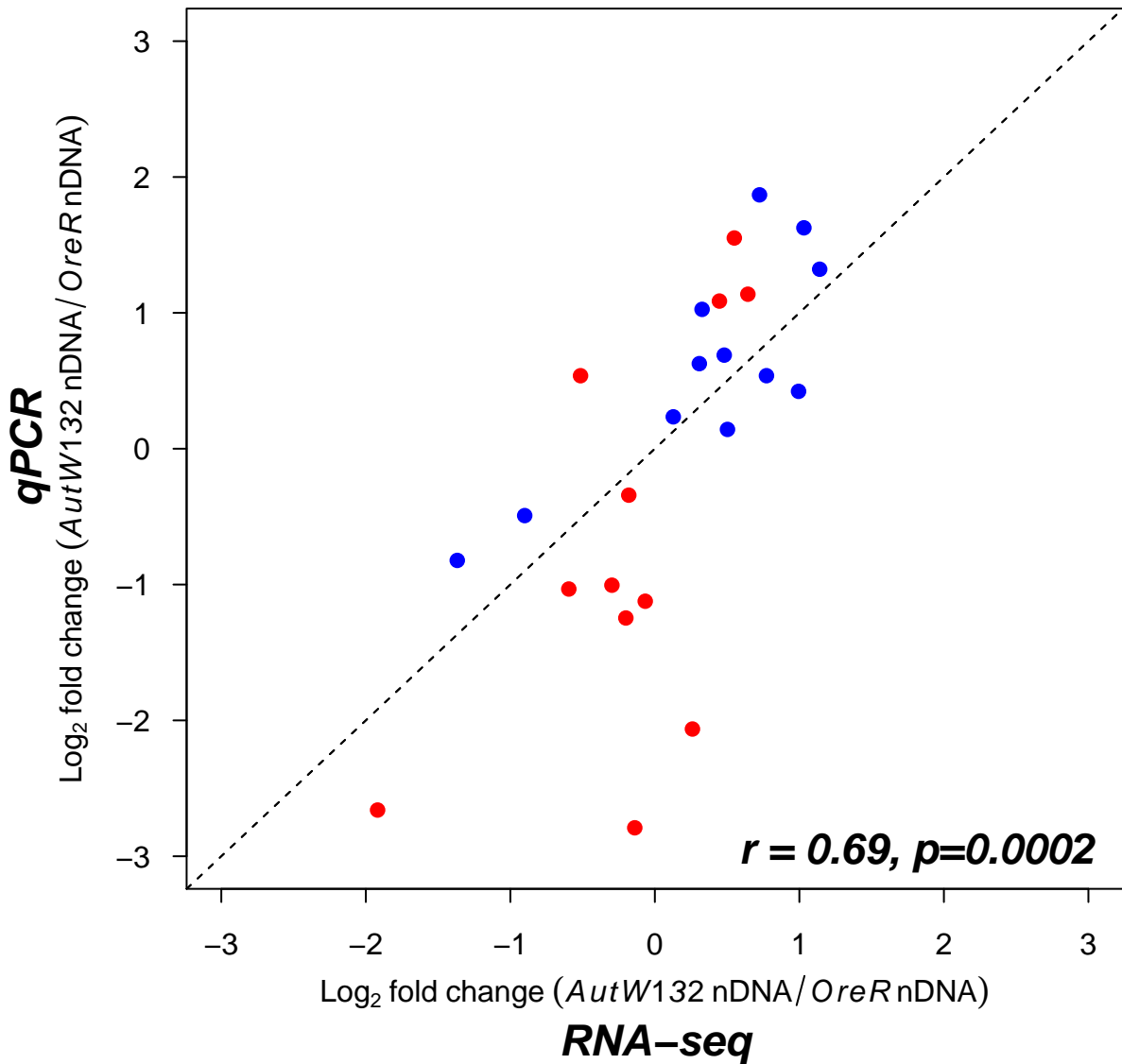
### mtDNA x nDNA



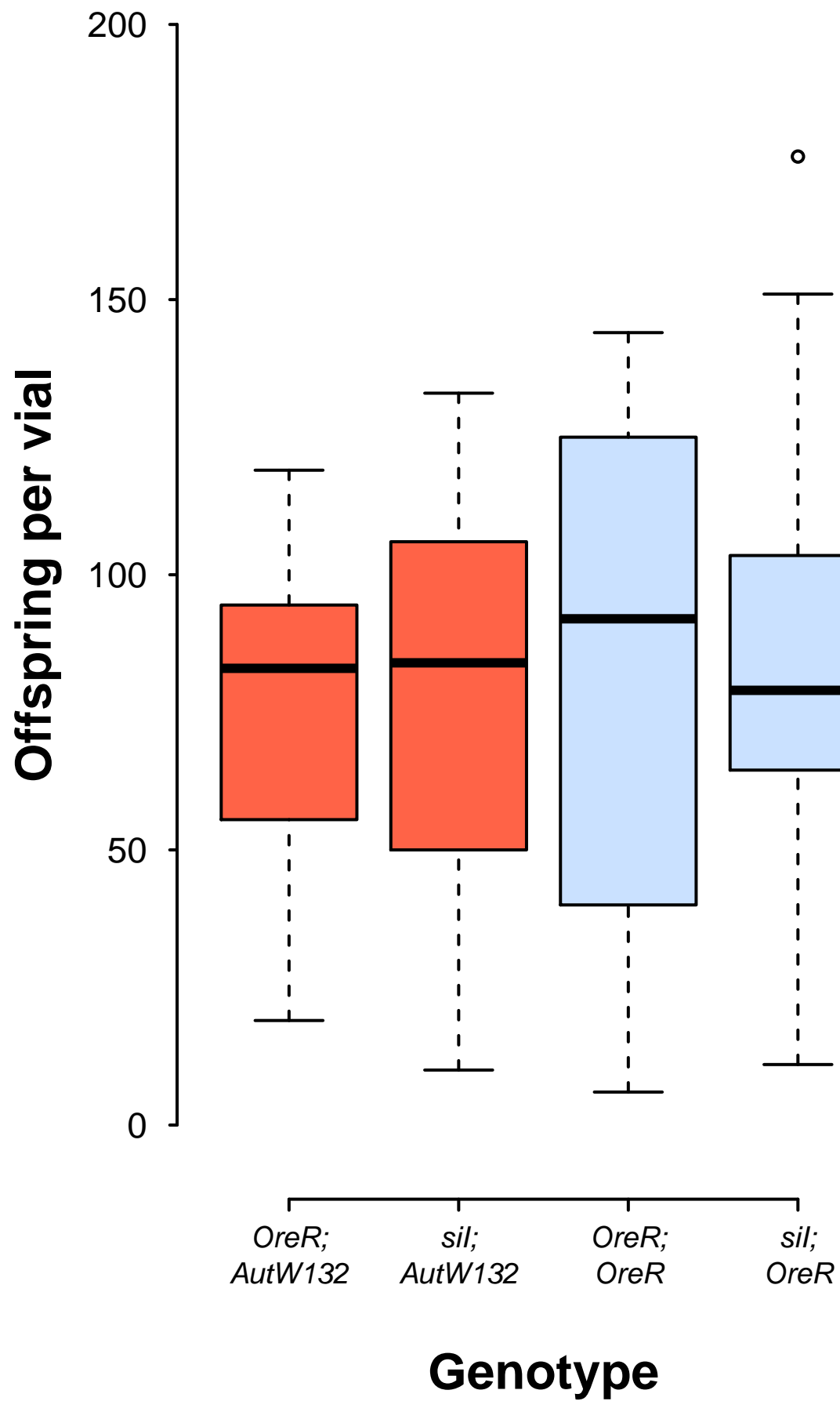
Computed gene ID	Flybase ID	Gene ID
CG10011	FBgn0039590	CG10011
CG10182	FBgn0039091	CG10182
CG10248	FBgn0013772	Cyp6a8
CG10275	FBgn0032683	kon
CG10623	FBgn0032727	CG10623
CG10799	FBgn0033821	CG10799
CG10816	FBgn0010388	Dro
CG10842	FBgn0015037	Cyp4p1
CG11263	FBgn0036330	CG11263
CG1131	FBgn0015569	alpha-Est10
CG1143	FBgn0035359	CG1143
CG11586	FBgn0035520	CG11586
CG1165	FBgn0004430	LysS
CG11752	FBgn0030292	CG11752
CG1179	FBgn0004425	LysB
CG1180	FBgn0004428	LysE
CG11966	FBgn0037645	CG11966
CG11985	FBgn0040534	CG11985
CG12400	FBgn0031505	ND-B14.5B
CG12763	FBgn0004240	DptA
CG12883	FBgn0039538	CG12883
CG12934	FBgn0033541	CG12934
CG13177	FBgn0040759	CG13177
CG13306	FBgn0040828	CG13306
CG13321	FBgn0033787	CG13321
CG13482	FBgn0036419	CG13482
CG13551	FBgn0040660	CG13551
CG13751	FBgn0033340	CG13751
CG14120	FBgn0036321	CG14120
CG14125	FBgn0036232	CG14125
CG14688	FBgn0037819	CG14688
CG14715	FBgn0037930	CG14715
CG14745	FBgn0043575	PGRP-SC2
CG14746	FBgn0043576	PGRP-SC1a
CG15065	FBgn0040734	CG15065
CG15066	FBgn0034328	IM23
CG15083	FBgn0034399	CG15083
CG15168	FBgn0032732	CG15168
CG15231	FBgn0040653	IM4
CG15534	FBgn0039769	CG15534
CG15707	FBgn0034098	krimp
CG15918	FBgn0034197	Cda9
CG1623	FBgn0033448	hebe
CG1648	FBgn0033446	CG1648
CG16725	FBgn0036641	Smn
CG16727	FBgn0038719	CG16727
CG17003	FBgn0031082	CG17003
CG17327	FBgn0038107	CG17327
CG17776	FBgn0040899	CG17776
CG1836	FBgn0026777	Rad23
CG18585	FBgn0031929	CG18585
CG18600	FBgn0038601	CG18600
CG18624	FBgn0029971	ND-MNLL
CG1981	FBgn0026869	Thd1
CG2065	FBgn0033204	CG2065
CG2083	FBgn0263392	Tet
CG2210	FBgn0000150	awd
CG2222	FBgn0030196	Psf3
CG30273	FBgn0050273	CG30273
CG30494	FBgn0263077	CG43340
CG3085	FBgn0034816	CG3085
CG31034	FBgn0003356	Jon99Cii
CG31089	FBgn0051089	CG31089
CG31148	FBgn0051148	Gba1a
CG31205	FBgn0051205	CG31205
CG31362	FBgn0003357	Jon99Ciii
CG31463	FBgn0051463	CG31463
CG32019	FBgn0005666	bt
CG32025	FBgn0266084	Fhos
CG32030	FBgn0266084	Fhos
CG32038	FBgn0266124	ghi
CG32557	FBgn0052557	CG32557
CG32599	FBgn0260482	CG32599
CG3264	FBgn0034712	CG3264
CG33002	FBgn0053002	mRpL27
CG33196	FBgn0053196	dpy
CG33256	FBgn0261565	Lmpt
CG33346	FBgn0053346	CG33346
CG3350	FBgn0039509	bigmax
CG33533	FBgn0053533	lectin-37Db
CG34073	FBgn0013672	mt:ATPase6
CG34083	FBgn0013684	mt:ND5
CG34089	FBgn0013685	mt:ND6
CG34212	FBgn0085241	CG34212
CG34227	FBgn0085256	CG34227
CG3683	FBgn0035046	ND-19
CG3759	FBgn0032116	Mco1
CG3939	FBgn0040396	CG3939
CG3986	FBgn0022700	Cht4
CG4000	FBgn0038820	CG4000
CG41421	FBgn0085643	CG41421
CG41536	FBgn0085675	CG41536
CG4178	FBgn0002563	Lsp1beta
CG42254	FBgn0259112	CR42254
CG4847	FBgn0034229	CG4847
CG4869	FBgn0003890	betaTub97EF
CG5242	FBgn0037892	mRpL40
CG5381	FBgn0032218	CG5381
CG5646	FBgn0039525	CG5646
CG5767	FBgn0034292	CG5767
CG5830	FBgn0036556	CG5830
CG6004	FBgn0036203	Muc68D
CG6272	FBgn0036126	CG6272
CG6503	FBgn0040606	CG6503
CG6602	FBgn0035673	CG6602
CG6620	FBgn0024227	aurB
CG6972	FBgn0039008	CG6972
CG7014	FBgn0038277	Rp55b
CG7068	FBgn0041181	Tep3
CG7291	FBgn0031381	Npc2a
CG7407	FBgn0037134	CG7407
CG7542	FBgn0036738	CG7542
CG7601	FBgn0027583	CG7601
CG7622	FBgn0002579	RpL36
CG8147	FBgn0043791	phu
CG8577	FBgn0033327	PGRP-SC1b
CG8958	FBgn0030725	CG8958
CG9025	FBgn0034542	Fem-1
CG9034	FBgn0040931	CG9034
CG9044	FBgn0031752	CG9044
CG9111	FBgn0004426	LysC
CG9116	FBgn0004429	LysP
CG9118	FBgn0004427	LysD
CG9450	FBgn0003891	tud



Log<sub>2</sub> fold change comparisons  
RNA-seq vs qPCR



**A** Females



**B** Males

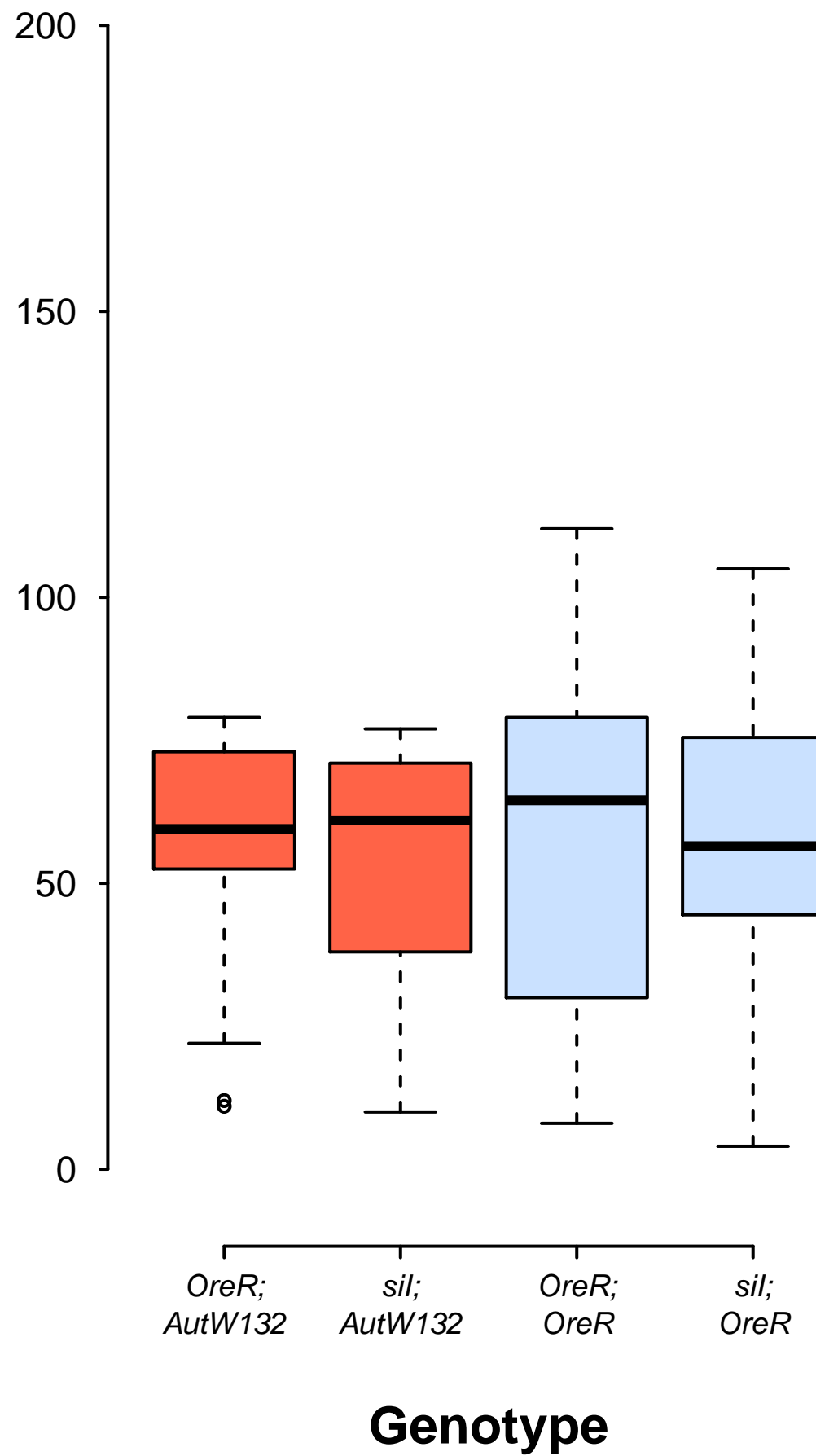


**Table S1. qPCR primers and sequences used in the RNA-seq validation.** Gene names, CG IDs and primer sequences are shown (5'->3' direction).

Gene name	Computed gene ID	Forward primer (5'->3')	Reverse primer (5'->3')
<i>RpL32 (rp49)</i>	CG7939	GATATGCTAAGCTGTCGCACAAA	TAACCGATGTTGGGCATCAGA
<i>Cox4A</i>	CG10664	CCAGCTTCTGCCAGACTATCG	GGCAGCTCATCGTACACGAA
<i>Cox5B</i>	CG11015	TGCATCTGCGAAGAGGATCA	TCTCCACCAGCTTGAACCAA
<i>Cox6B</i>	CG14235	TCGACCCACGGTTCCCTAA	GCACATCGACTTGTAGACCTTCTG
<i>Cox7AL</i>	CG18193	CCGAAGACACGTCCCTGGAA	TGTTATCCATACTGCCGCCTTT
<i>Cox8</i>	CG7181	CATCTCCACCGCCGAGAA	TTGTAGTCCCGGATGTGGTAGA
<i>Hsp68</i>	CG5436	AACTGGAGACCTATTTGTTTGG	CCTTCAGTTTGTACTCGTACTC

**Table S2. Generalized linear models of offspring production in females (analysis of deviance).** Terms in the model were nDNA type, mtDNA type, and block. All first order effects and interaction terms were fitted. We report the degrees-of-freedom (df), deviance, residual degrees-of-freedom, residual deviance and p-values based on a Chi-squared distribution. P-values in bold are significant at  $\alpha=0.05$ .

<b>Model term</b>	<b>df</b>	<b>Deviance</b>	<b>Residual df</b>	<b>Residual deviance</b>	<b>P (&gt;Chi)</b>
	-	-	92	148.51	-
nDNA	1	0.84	91	147.67	0.36
mtDNA	1	0.23	90	147.45	0.63
Block	1	44.96	89	102.49	<b>2.014E-11</b>
nDNA x mtDNA	1	0.54	88	101.95	0.46
nDNA x block	1	0.31	87	101.64	0.58
mtDNA x block	1	0.17	86	101.47	0.68
nDNA x mtDNA x block	1	2.01	85	99.46	0.16

**Table S3. Generalized linear models of offspring production in males (analysis of deviance).** Terms in the model were nDNA type, mtDNA type, and block. All first order effects and interaction terms were fitted. We report the degrees-of-freedom (df), deviance, residual degrees-of-freedom, residual deviance and p-values based on a Chi-squared distribution. P-values in bold are significant at  $\alpha=0.05$ .

<b>Model term</b>	<b>df</b>		<b>Residual deviance</b>		<b>P (&gt;Chi)</b>
	-	-	92	130.25	-
nDNA	1	0.65	91	129.60	0.42
mtDNA	1	0.03	90	129.58	0.87
Block	1	26.71	89	102.87	<b>2.368E-07</b>
nDNA x mtDNA	1	1.18	88	101.68	0.28
nDNA x block	1	0.68	87	101.00	0.41
mtDNA x block	1	0.22	86	100.78	0.64
nDNA x mtDNA x block	1	0.96	85	99.82	0.33

# Supporting Information

## Mitochondrial-nuclear interactions mediate sex-specific transcriptional profiles in *Drosophila*

Mossman JA, Tross JG, Li N, Wu Z, Rand DM

### qPCR validation of RNA-seq data obtained on an Illumina Hiseq 2000 platform

To validate transcription expression measurements, we conducted qPCR on seven primer pairs to determine if the RNA-seq data showed qualitatively and quantitatively similar results to those obtained by qPCR. We aimed to test whether the  $\log_2$ -fold changes obtained on the RNA-seq platform (Illumina Hiseq 2000, Illumina, Inc, CA, USA) were similar to those from qPCR (Applied Biosystems™ 7300 Real Time PCR System, Applied Biosystems, ThermoFisher Scientific, MA, USA).

The accuracy of qPCR depends on the magnitude of log fold change between the contrasting treatments and small fold changes can be difficult to interpret (MOREY *et al.* 2006). Since the mtDNA effects we observed for nuclear genes were small in magnitude, we used the contrast between nuclear backgrounds within a mitochondrial haplotype to validate the expression results. This was done for both mtDNA haplotypes and the contrast was the effect of *AutW132* nuclear background relative to the *Oregon R* nuclear background.

MtDNA primers for qPCR for the two mtDNA haplotypes we studied are problematic to design because of the high A+T content of *Drosophila* mtDNA and the haplotype variation between *D. melanogaster* and *D. simulans* mtDNA introduces SNPs into useful primer sequences and differential expression cannot be easily teased apart from differential annealing efficiency. To circumvent this problem, we focused on nuclear genes that encode mitochondrial protein products in cytochrome c oxidase (complex IV of the electron transport chain), along with heat shock protein 68 (*hsp68*). These genes showed differences in expression between nuclear backgrounds, as judged by read counts from RNA-seq. We also measured a

reference housekeeping gene: Ribosomal protein L32 (*rp49*), which was used as an internal control for RNA concentration. A list of primers and primer sequences are shown in Table S1. Two biological replicates of each genotype were measured, with triplicate technical replicates, totaling 96 PCRs for each gene of interest (48x 'focal' gene and 48x 'internal *rp49* controls'). Conducting the qPCRs in this way prevented comparison across plates for a focal gene. Negative samples were run on a separate plate. All negative samples showed no detectable values of fluorescence.

**Table S1. qPCR primers and sequences used in the RNA-seq validation.** Gene names, CG IDs and primer sequences are shown (5'->3' direction).

Gene name	Computed gene ID	Forward primer (5'->3')	Reverse primer (5'->3')
<i>RpL32 (rp49)</i>	CG7939	GATATGCTAAGCTGTGCGACAAA	TAACCGATGTTGGGCATCAGA
<i>Cox4A</i>	CG10664	CCAGCTTCTGCCAGACTATCG	GGCAGCTCATCGTACACGAA
<i>Cox5B</i>	CG11015	TGCATCTGCGAAGAGGATCA	TCTCCACCAGCTTGAACCAA
<i>Cox6B</i>	CG14235	TCGACCCACGGTTCCCTAA	GCACATCGACTTGTAGACCTTCTG
<i>Cox7AL</i>	CG18193	CCGAAGACACGTCTCTGGAA	TGTTATCCATACTGCCGCCTTT
<i>Cox8</i>	CG7181	CATCTCCACCGCCGAGAA	TTGTAGTCCCGGATGTGGTAGA
<i>Hsp68</i>	CG5436	AACTGGAGACCTATTTGTTTGG	CCTTCAGTTGTACTCGTACTC

To obtain relevant RNA-seq values, we conducted separate DESeq (ANDERS and HUBER 2010) analyses using the same two biological replicates as used in the qPCR with the contrast between nuclear backgrounds. The log<sub>2</sub>-fold changes for the focal genes were used as comparison in the qPCR-RNA-seq correlation.

qPCRs were conducted using Power SYBR<sup>®</sup> Green system (Applied Biosystems, CA, USA) using a two-step protocol. We used the same mRNA template that was used in the main Illumina RNA-seq study.

#### *DNase treatment*

Briefly, 44µl mRNA + H<sub>2</sub>O were mixed with 5µl 10x Turbo DNase buffer (Invitrogen, ThermoFisher Scientific, MA, USA) and 1µl Turbo DNase (Invitrogen, ThermoFisher Scientific, MA, USA) to remove any contaminating DNA. After 30 minutes of incubation at 37°C, an additional 1µl of DNase was added and

this mixture was further incubated for 30 minutes at 37°C. Following, we added 10µl of DNase inactivation buffer (Invitrogen, ThermoFisher Scientific, MA, USA), which was mixed then centrifuged. The supernatant was aspirated, then re-centrifuged. The supernatant from the second centrifugation was the template for cDNA synthesis.

#### *cDNA synthesis*

We quantified the RNA concentration using a Nanodrop (ThermoFisher Scientific, MA, USA) and standardized to 5ng/µl. 15µl of 5ng/µl RNA solution was added to 4µl iScript cDNA synthesis reaction mixture (Bio-Rad Laboratories, Inc, CA, USA) and 1µl reverse transcriptase (Bio-Rad Laboratories, Inc, CA, USA). cDNA synthesis was carried out using the following thermocycling protocol: 5 minutes at 25°C, 30 minutes at 42°C, then 5 minutes at 85°C. cDNA concentration was measured using a Nanodrop and diluted to a standard concentration (120ng/µl). qPCR was conducted on the cDNAs using the following reaction mixture: 10µl SYBR Green reaction mixture, 0.5µl of each primer (at 50 pmol/µl concentration), 6µl H<sub>2</sub>O, and 3µl cDNA.

#### *qPCR*

qPCR was conducted using an Applied Biosystems 7300 Real Time PCR System (Applied Biosystems, ThermoFisher Scientific, MA, USA). The thermocycling protocol was as follows: an initial incubation at 50°C (2 minutes), followed by 95°C (10 minutes), then 40 cycles of 95°C (15 seconds) → 60°C (60 seconds). A dissociation step was added: (95°C, 15 seconds), followed by 60°C (1 minute), 95°C (15 seconds), then 60°C (15 seconds). Melting curves were checked for primer dimers and none were detected. Amplification curves were analyzed using Applied Biosystems Sequence Detection Software v1.4.0.27, with the auto C<sub>T</sub> function.

#### *Log<sub>2</sub>-fold changes*



For each focal gene, we assessed  $\log_2$ -fold changes of *AutW132* nuclear background against the *Oregon R* reference using the comparative threshold cycle,  $C_T$ , method ( $2^{-\Delta\Delta C_T}$ ) (SCHMITTGEN and LIVAK 2008), with samples standardized to the *rp49* gene reference (internal control). We estimated the  $\log_2$ -fold difference against each biological replicate ‘calibrator’, and used the mean value of these two measures in the correlation analysis.

In total, we correlated 24 samples (4x genotypes, 6x genes) and found a significant positive correlation between  $\log_2$ -fold change estimated by RNA-seq and qPCR ( $r=0.69$ ,  $t = 4.52$ ,  $df=22$ ,  $p=0.00016$ : Figure S13). When the data were parsed into female and male datasets- the red and blue data in Figure S13, respectively- both subsets demonstrated significant positive correlations between measurement estimates; female correlation:  $r= 0.60$ ,  $t= 2.40$ ,  $df= 10$ ,  $p= 0.037$ ; male correlation:  $r= 0.81$ ,  $t=4.375$ ,  $df=10$ ,  $p= 0.001$ .

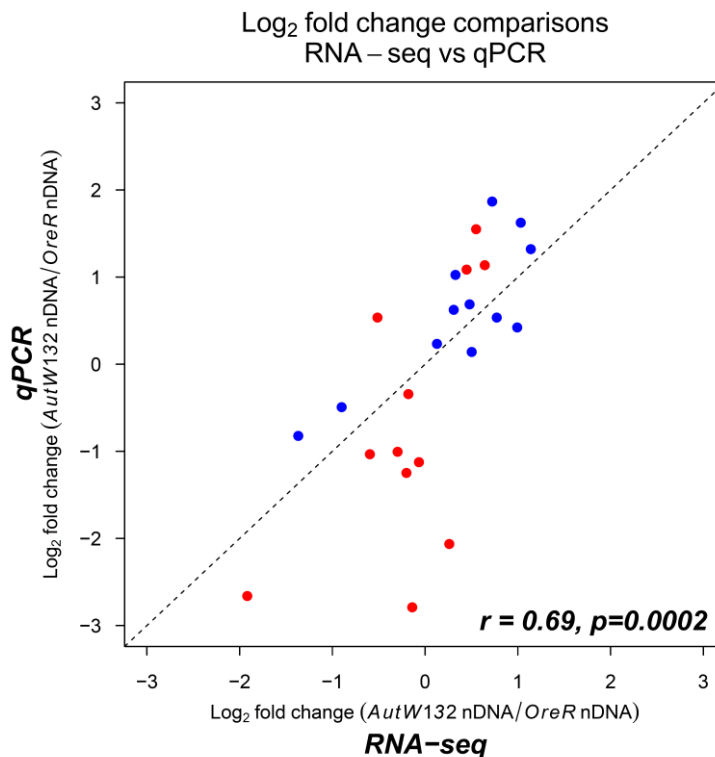


**Figure S13. Correlation between RNA-seq and qPCR estimates of  $\log_2$ -fold change.** Data from all 4 mitonuclear genotypes across 6 nuclear loci are shown. Samples in blue are male genotypes, samples in red are female genotypes.  $\log_2$ -fold change estimates were judged using the  $\Delta\Delta C_T$  method (qPCR) and

DESeq (RNA-seq). The genotype contrasts are between *AutW132* and *Oregon R (OreR)* in both mtDNA backgrounds (*sil* and *Oregon R*). The dashed line shows  $\log_2$ -fold change equality between the expression measurement platforms.

### Offspring production in the mitonuclear genotype panel

We used results from a previous study (MONTTOOTH *et al.* 2010) to investigate whether there were differences in fecundity between the genotypes for females and males. Full details on the materials and methods for this assay can be found in (MONTTOOTH *et al.* 2010). Briefly, we summed the total number of offspring that were produced in a fitness assay. The assay consisted of six replicate vials of five females and five males that were allowed to continually mate and lay eggs for two days. Each set of parents were flipped onto fresh food after two days, for a total of 12 days, giving six two-day broods. Each genotype x sex combination (individual boxes in Figure S14) represents 11-12 vials. Figure S14 describes these data.

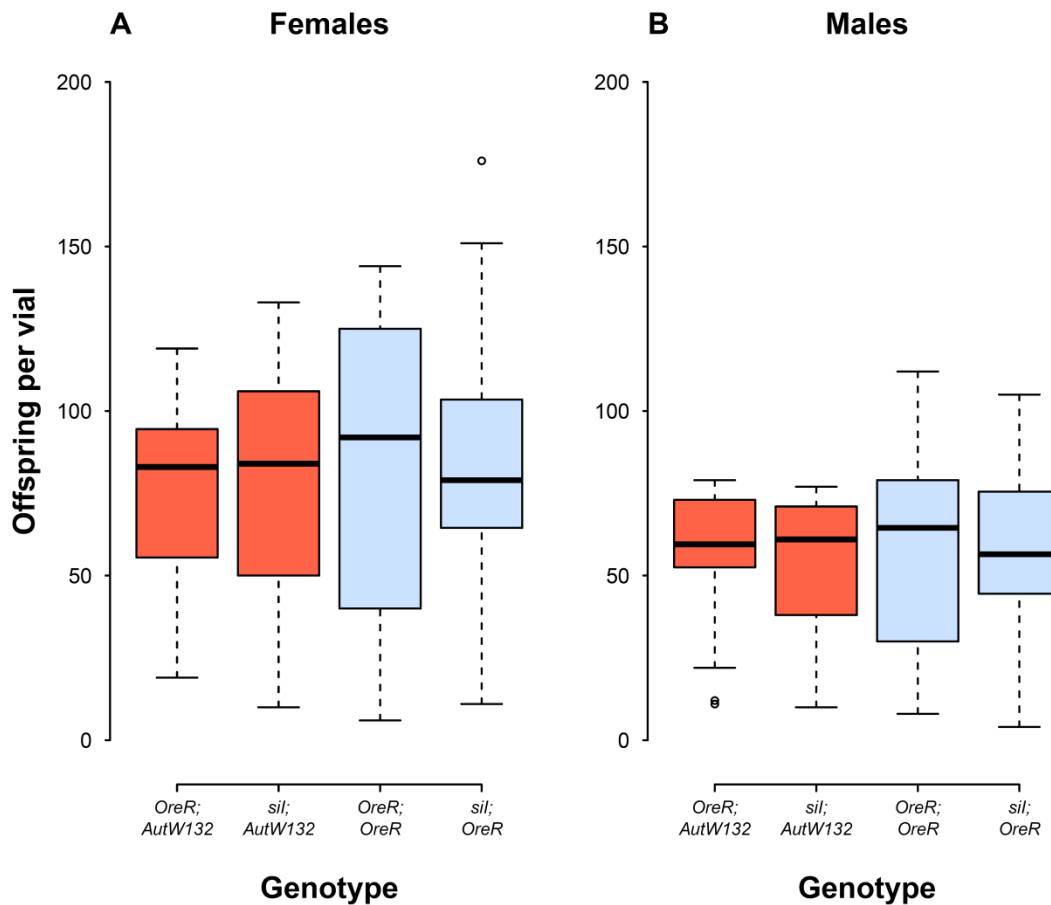


**Figure S14. Offspring production within the four genotypes used in this study.** Female (A) and male (B) results are shown. The two nuclear backgrounds are distinguished by color; *AutW132* (orange) and *OreR* (blue). Data are from (MONTTOOTH *et al.* 2010). Within each sex there were no significant main effects of nuclear background or mtDNA haplotype on offspring numbers, and their interaction was not significant (see Tables S2 and S3 for the female and male results, respectively). The *mito;nuclear* genotypes are labeled on the abscissa.

We tested whether nuclear background, mtDNA haplotype, or their interaction were significantly associated with the number of offspring. The offspring numbers per vial were (overdispersed) count data and we therefore used a negative binomial error structure with log-link function in generalized linear models. We confirmed the analyses results using a quasipoisson error and the results were qualitatively identical. Here, we report only the results of the negative binomial models. The offspring number estimates were conducted in two separate blocks and we therefore fit ‘block’ as a term in our models.

Across all model terms, block as a first order effect was the only significant association with offspring numbers in females (Table S2) and males (Table S3). nDNA, mtDNA, and their nDNA x mtDNA interaction were non-significant terms. Interactions between mtDNA and nDNA with block, along with the 3-way interaction (mtDNA x nDNA x block) were non-significant in both sexes. These results demonstrate that mtDNA and nDNA, along with their interaction are not associated with offspring numbers – our measure of fecundity- in this genotype panel. It also confirms that first and second order effects were not different between the blocks.

**Table S2. Generalized linear models of offspring production in females (analysis of deviance).** Terms in the model were nDNA type, mtDNA type, and block. All first order effects and interaction terms were fitted. We report the degrees-of-freedom (df), deviance, residual degrees-of-freedom, residual deviance and p-values based on a Chi-squared distribution. P-values in bold are significant at  $\alpha=0.05$ .

Model term	df	Deviance	Residual df	Residual deviance	P (>Chi)
	-	-	92	148.51	-
nDNA	1	0.84	91	147.67	0.36
mtDNA	1	0.23	90	147.45	0.63
Block	1	44.96	89	102.49	<b>2.014E-11</b>
nDNA x mtDNA	1	0.54	88	101.95	0.46
nDNA x block	1	0.31	87	101.64	0.58
mtDNA x block	1	0.17	86	101.47	0.68
nDNA x mtDNA x block	1	2.01	85	99.46	0.16

**Table S3. Generalized linear models of offspring production in males (analysis of deviance).** Terms in the model were nDNA type, mtDNA type, and block. All first order effects and interaction terms were fitted. We report the degrees-of-freedom (df), deviance, residual degrees-of-freedom, residual deviance and p-values based on a Chi-squared distribution. P-values in bold are significant at  $\alpha=0.05$ .

Model term	df	Deviance	Residual df	Residual deviance	P (>Chi)
	-	-	92	130.25	-
nDNA	1	0.65	91	129.60	0.42
mtDNA	1	0.03	90	129.58	0.87
Block	1	26.71	89	102.87	<b>2.368E-07</b>
nDNA x mtDNA	1	1.18	88	101.68	0.28
nDNA x block	1	0.68	87	101.00	0.41
mtDNA x block	1	0.22	86	100.78	0.64
nDNA x mtDNA x block	1	0.96	85	99.82	0.33

## Supporting References

- ANDERS, S., and W. HUBER, 2010 Differential expression analysis for sequence count data. *Genome Biology* **11**: 1-12.
- MONTOOTH, K. L., C. D. MEIKLEJOHN, D. N. ABT and D. M. RAND, 2010 Mitochondrial-nuclear epistasis affects fitness within species but does not contribute to fixed incompatibilities between species of *Drosophila*. *Evolution* **64**: 3364-3379.
- MOREY, J. S., J. C. RYAN and F. M. VAN DOLAH, 2006 Microarray validation: factors influencing correlation between oligonucleotide microarrays and real-time PCR. *Biological Procedures Online* **8**: 175-193.
- SCHMITTGEN, T. D., and K. J. LIVAK, 2008 Analyzing real-time PCR data by the comparative CT method. *Nat. Protocols* **3**: 1101-1108.